ROYAL SOCIETY
OF CHEMISTRY

Check for updates

Review on polyaniline-based nanocomposite heterogeneous catalysts for catalytic reduction of hazardous water pollutants

Parmeshwar Lal Meena [ID] * and Ajay Kumar Surela

Water contamination by highly toxic substances has generated serious ecological disturbances and health problems for humans. Hence, decontamination of toxic pollutants using advanced, inexpensive, and eco-friendly approaches is the current demand. Heterogeneous catalyst-based catalytic reduction processes have offered the opportunity to transform hazardous water pollutants into non-hazardous products *via* sustainable, eco-friendly, and efficient routes and might be a competitive substitute for existing traditional water purification techniques. However, the key challenges linked with pure heterogeneous catalysts include agglomeration and poor dispersion, stability, recovery, and reusability, which result in poor activity and efficiency. Thus, it is essential to produce multipurpose polymer-based composite catalysts using conducting polymers, which are exceptionally good supportive and matrix materials. The blending of metal-based nanomaterials with polyaniline conducting polymers produces highly stable and efficient heterogeneous nanocomposite catalysts with amazing catalytic activity against a wide range of water pollutants. The heterogeneous catalytic reductive degradation of immensely toxic pollutant water has gained substantial curiosity because of its excellent physicochemical and surface characteristics, porous structure, recoverability, and recyclability. Therefore, this review presents the latest efforts to generate various polyaniline-based nanocomposite catalysts using a polyaniline matrix and various nanofiller materials and their potential applications in heterogeneous catalytic reduction degradation of water pollutants.

1. Introduction

Water does not have any nutritional value but is essential for the survival of all living creatures. Currently, water shortage and purity have become critical and challenging tasks worldwide. However, 70% of Earth is covered with water, but approximately 3% of this water is fresh and adequate for drinking.[1–3] The fast-growing population across the globe and intensified level of industrial and urban activities have introduced a new stage of stress to the supply of fresh water.[4,5] It is estimated that by 2025, approximately 50% of the total global population will struggle for drinking water.[2] Moreover, the continuous decline of water quantity and quality has significantly influenced the advantageous applications of water. This has demanded highly efficient, inexpensive, eco-friendly, and effective water purification processes to discard toxic water pollutants and improve water quality to the recommended levels of regulatory bodies. It is observed that traditional water treatment processes are mainly designed to remove bio-organisms such as bacteria, viruses, and protozoans or inactivate them using chemicals to trim down the threats of water-borne diseases.[2] However, various

challenges are still associated with the above-mentioned techniques. For instance, physical treatment methods, such as adsorption and air stripping processes generate waste or sludge, which needs to be further treated, and in chemical methods, the formation of toxic byproducts is a significant issue due to poor selectivity for targeted pollutants.[6,7] Biological methods consume a longer time; however, they are widely employed and maintain a long-term activity.[8] Additionally, the toxicity of discharged pollutants inhibits the activity of biological processes in some cases.[9] The limitations associated with traditional methods and the progressive contraction of water standards and guidelines[10] have inspired research communities to discover new, green, and efficient water treatment methods.

Compared to the traditional approaches for water treatment, the use of advanced reduction techniques (ARTs), which include the catalytic reduction of pollutants, is favored to convert highly toxic pollutants into less hazardous or nonhazardous products.[2] The reductive degradation is one the most efficient and significant traditional processes to eliminate the noxious and carcinogenic pollutants from polluted water.[11,12] However, catalysis is largely concerned with the chemical industry but not as a water treatment technique.[2] Currently, the catalytic reduction method of water purification is widely investigated at the laboratory and field scale and displayed thrilling results in both

Department of Chemistry, University of Rajasthan, Jaipur 302004, India. E-mail: parmeshwar1978@gmail.com

groundwater and industrial wastewater treatments.[13] The chemical reduction process shows better activity and greater selectivity, generates less or non-toxic products and more eagerly eco-friendly products,[14] and consumes fewer reagents.[2] Based on the physical state of the utilized catalyst, the catalytic reduction process can be categorized as a homogeneously and heterogeneously catalyzed reduction process; when the solid catalyst is utilized, it is called heterogeneous catalytic reduction,[15] and in homogeneous catalysis, a liquid phase catalyst is utilized. Usually, heterogeneous catalysis in water treatment is preferred because the isolation of the utilized catalyst in homogenous catalysis of water pollutants is technically and/or economically unfeasible and the soluble catalyst can generate serious ecological issues. In heterogeneous catalysis, the catalyst can be recovered *via* filtration, centrifugation, or other approaches easily, and a small amount of catalyst can effectively speed up the water purification process.[16] The commonly explored heterogeneous nano-catalysts in catalytic reduction processes are metal-based nanomaterials that exhibit extraordinary reduction potential against various water pollutants under normal reaction conditions. However, pure metal-based catalysts (metal and metal oxide NPs) suffer from serious drawbacks, such as poor stability, aggregation, dispersion, recovery, and reusability. Hence, to overcome these limitations and advance the characteristics of pure catalysts, they are immobilized and blended with effective supporting materials, such as polymers, carbon-based materials, and silica. Among polymers, conducting polymers (CPs) have been extensively explored as supporting materials for numerous nanomaterials. Polyaniline (PANI) is a well-known CP with distinctive combinational features because of its effective electronic characteristics and good chemical and photostability, making it a suitable candidate for various uses in multi-disciplinary fields.[17,18] Using PANI as a supporting matrix or shelter to various nanomaterials, different types of binary, ternary, and quaternary heterogeneous catalysts have been produced with significantly improved features and effectively utilized for the catalytic degradation of various water pollutants in the presence of a reducing agent. The current review presents the categorization of PANI nanocomposites as binary, ternary, and quaternary composites (Fig. 1), their synthesis utilizing different synthesis techniques, and their application as heterogeneous catalysts for the catalytic reduction degradation of various toxic water pollutants. Moreover, this review study will help in understudying new findings of the heterogeneous catalysis process, adding new aspects to the literature, and presenting information to the public to thrill them for the potential practical application of this technique for water treatment.

2. Characteristics of polyaniline and its synthesis

Historically, PANI was first prepared 190 years ago in 1834 by heating aniline nitrate with $CuCl_2$ at 100 °C on a porcelain plate.[19] Since then, it has become the most widely studied conducting polymer due to its facile and simple preparation
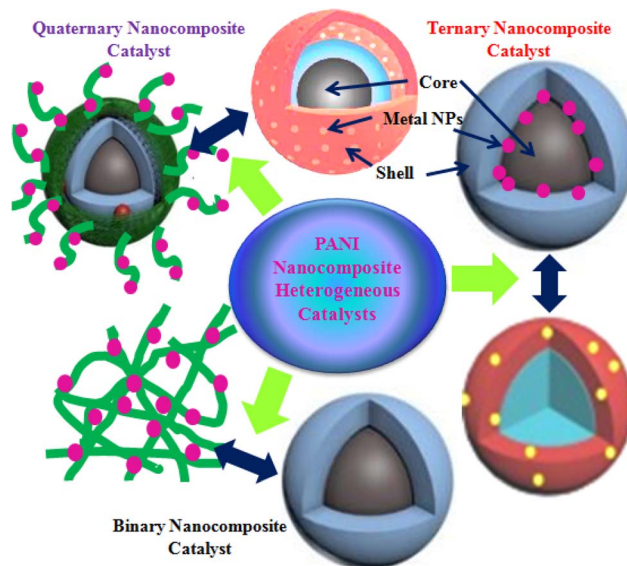

Fig. 1 Different types of polyaniline nanocomposite heterogeneous catalysts.

process,[20] and extensive acid–base doping and dedoping ability.[21] PANI is a heterogeneous and semi-crystalline polymer in which an ordered section (crystalline) is dispersed in a disordered section (amorphous). The crystalline part is conducting and metallic, whereas the amorphous part is non-conducting and nonmetallic, and the crystalline region is accountable for the conducting nature of PANI.[22] PANI is a homopolymer of aniline monomer that exists in three basic forms, which are structurally differing and show different oxidation states. These states are leucoemeraldine base (LEB), emeraldine base (EB), and pernigraniline (PNB) (Scheme 1). The PANI backbone structurally consists of aromatic diamine functionalities quinoid and benzenoid in a well-ordered manner. Among the PANI forms, the emeraldine form
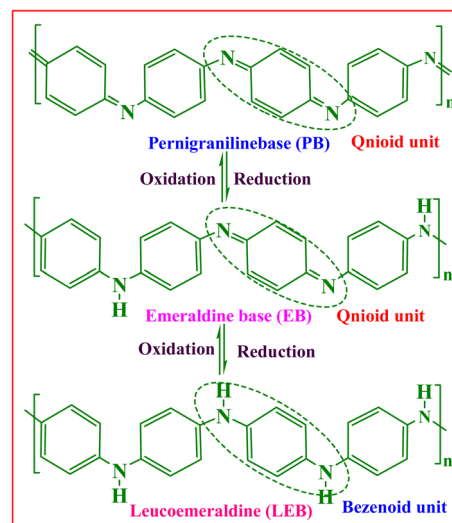
Scheme 1 Various forms of polyaniline showing benzoid and quinoid units.

consists of both benzoid and quinoid units, half oxidized, neutral in undoped form while cationic in doped form, and has polaron and bipolaron structures.[23] It is regarded as most suitable for doping due to its higher stability.[24] The leucoemeraldine form is completely reduced and structurally consists of benzoid units, and pernigraniline is fully oxidized and consists of benzoid and quinoid units.[23] The acid doping or protonation of EB produces polaron or bipolaron structures.[25]

PANI is prepared *via* polymerization of an aniline monomer using various methods. Frequently, the method used for PANI synthesis is chemical oxidative polymerization (COP) of aniline in an acidic medium, using various oxidizing agents, and acids (organic or inorganic acids) as dopants. The most frequently employed oxidizing agents are ammonium persulphate (APS: $(NH_4)_2S_2O_8$) and Fe(III). However, other oxidizing agents such as transition metal ions, such as Mn^{3+}, Mn^{6+}, Mn^{7+}, Cr^{6+}, Ce^{4+}, V^{5+}, and Cu^{2+}; noble metal compounds, such as Au^{3+}, Pt^{6+}, Pd^{2+}, Ag^+, KIO_3, H_2O_2, and benzoyl peroxide; a mixture of oxidants $FeCl_3/H_2O_2$ and $KIO_3/NaClO$; *in situ* produced oxidants (Mo^{5+} compounds); enzymes such as horseradish peroxidase and oxidoreductase with H_2O_2; laccase with $K_3[Mo(CN)_8]$; and Fe(II) salts are also utilized.[21] Through this procedure, PANI is obtained in the precipitate (solid powdered) form in morphologically different nanostructures, such as fiber, particle, sphere, rod, sheet, thread, tube, and micelle flower. The oxidation of aniline is influenced by several factors, such as concentration of oxidant, concentration of monomer, reaction medium, duration of the reaction, and temperature.[26]

Besides this procedure, other methods are also employed for the synthesis of PANI, including solid-state polymerization,[27,28] electroless polymerization,[29] electrochemical oxidative polymerization,[30,31] plasma polymerization,[32] sonochemical,[33] photoinduced polymerization,[34] solution polymerization,[35] colloidal dispersion polymerization,[22] seed polymerization,[36] self-assembling polymerization,[37] metathesis polymerization,[38] interfacial polymerization,[39,40] template synthesis,[41,42] enzymatic synthesis,[43] and emulsion polymerization,[44] as shown in Table 1. The electrochemical oxidative polymerization (EOP) procedure is carried out by passing an electric current through an inert electrode immersed in an acidic aniline solution in which polymerization of monomers occurs on the surface of the cationic electrode as a thin film. The EOP process of aniline is usually performed under constant conditions of potential (potentiostatic), current (galvanostatic), and potential sweeping/scanning. The electrode (anode) material utilized is Pt or glass,[22] and many other materials, such as Fe,[47] Cu,[48] Au,[49] graphite,[25] vitreous carbon,[50] and stainless steel[22,51] are also explored as electrode materials in the EOP process of PANI synthesis.

3. Synthesis of polyaniline nanocomposites

Usually, polymer-based nanocomposite formation is carried out using *in situ* or *ex situ* polymerization procedures,[52] as shown in Fig. 2. The *in situ* process includes the synthesis of a composite simultaneously combining the filler nanomaterial and polymerization of the monomer because the nanomaterials are excellently dispersed in the matrix phase, while in *ex situ* polymerization already prepared PANI is mixed with nanomaterials.[53] Thus, in the *ex situ* process, nanocomposites are prepared with poor dispersion, lower density, and non-uniform distribution of particles in the matrix,[52] while in the *in situ* process, homogeneously dispersed composites with a higher density are prepared. During the synthesis process, the nanocomposite particles can be adorned at the surface of the polymer or immobilized in the polymer matrix.[54] The deposition of nanomaterials on the surface of the polymer is cost-effective, creates higher active sites, improves surface properties, and reduces particle agglomeration, and it can be achieved *via* plasma polymerization, chemical vapor deposition, grafting, and dip-coating processes; however, there is a greater possibility of leaching of nanomaterial particles.[55–58]

Although the distribution of nanoparticles inside the polymer matrix reduces the leaching of particles from the matrix and improves the recoverability of particles, agglomeration may be higher,[54,58] and it can be achieved *via in situ* techniques that may be *in situ* polymerization or sol–gel process.[59] The *in situ* polymerization process entails a controlled immobilization of elected nanomaterial with the pure monomer solution before succeeding polymerization.[54] Except *in situ* and *ex situ* routes, physical mixing of polymeric structure (such as PANI) and nanomaterials already prepared are mixed by milling, solution, or melt mixing procedures. However, the components in the nanocomposite materials derived through this method are associated with weak physical interactions and thus possess poor attractions. All the processes adopted for the synthesis of PANI-nanocomposites are based on these three synthesis routes. The commonly employed synthesis methods of PANI-nanocomposites are summarized in Table 2.

4. PANI nanocomposite heterogeneous catalysts for degradation of water pollutants

Several contemporary studies have discovered that homogenous and heterogeneous catalysis processes are incredibly competent in eradicating pollutants.[70–72] In the homogenous or heterogeneous catalytic reduction process of various environmental pollutants, metal complexes or metal nanoparticles, particularly noble metal NPs, are usually employed.[73,74] Although in comparison to homogenous catalysts, the heterogeneous catalysts are more significant due to their non-solubility in solvents, providing wide surface support to reactants, greater stability, and good reusability.[75]

Due to a higher surface-to-volume quotient, the metal NPs show the unique ability of heterogeneous and homogenous catalysis potential during catalysis reactions. Heterogeneous catalysts display good revitalization and reusability features, while homogeneous catalysis shows excellent selectivity and comparatively small catalyst loadings.[76] Therefore, in many catalysis reactions, the applicability of metal NPs significantly

Table 1 Synthesis procedure for polyaniline

Synthesis technique	Description	References
Colloidal dispersion polymerization	Aniline polymerization produces a water-soluble polymer, which produces colloidal PANI particles instead of precipitation. Macroscopic precipitation is prevented by using a steric stabilizer	22
Solid state polymerization	Polymerization of aniline at the solid surface occurs on the surface of reactant molecules	27 and 28
Electroless polymerization	Polymerization of aniline without applying external potential in the acid medium in the metal surface (Pt, Pd) *via* an electrochemical pathway in which reduction of dissolved O_2 and oxidation of aniline take place *via* cathodic and anodic half-reactions, respectively, at the interface of metal/solution	29
Electrochemical oxidative polymerization	Aniline polymerization in an acidic solution by passing of current without using an oxidant produces homogeneous and pure products as film	30 and 31
Plasma polymerization	Injection of aniline in plasma produced by a DC glow discharge in which electrons or ions present in plasma induce polymerization, and polymerization takes place in solvent and chemical oxidant-free conditions	32
Sonochemical	Polymerization of aniline with drop-wise addition of oxidant under ultrasonic irradiation conditions produces PANI with higher solubility and scalability	33
Photoinduced polymerization	Polymerization of aniline in the presence of transition metal salts on illumination with light radiation produces PANI in composite form	34
Solution polymerization	Electo- or chemical polymerization of aniline in the solvent in which the produced PANI is obtained in solution form	35
Seed polymerization	Polymerization of aniline is carried out in the presence of foreign material (seed)	36
Self-assembling polymerization	Polymerization of aniline vapor on oxidant-coated substrate surface as PANI film	37
Metathesis polymerization	Obtaining PANI without using aniline by heating 1,4-dichlorobenzene in organic solvent (benzene) for 12 h at 220 °C with sodium amide	38
Interfacial polymerization	Aniline polymerization is carried out at the interface of two immiscible solvents using acid dopant and oxidant with a construable and slow polymerization rate	39 and 40
Template synthesis	Polymerization of monomer into the polymer in compliance with information received from the template present in the reaction mixture	41 and 42
Enzymatic synthesis	Polymerization of aniline is carried out by enzyme at low temperature and neutral pH producing small chain length PANI with a lower degree of doping	43
Emulsion polymerization	Polymerization of monomer in a water-dispersed phase which is dispersed in an aqueous phase that contains a surfactant	44
Chemical oxidative polymerization	Polymerization of aniline monomer is initiated by a chemical oxidant in an acidic solution that produces a bulk product in a short time	45 and 46

increased in current times,[77] and in catalysis processes, the use of metal nanoparticles stems as a potential contender in various catalytic reactions due to their remarkable catalytic potential owing to specific crystalline features and higher specific surface area.[78] However, the high surface area and surface energy due to their small size enable them to form aggregates and generate large-sized particles so that they can minimize surface energy, which accordingly reduces their catalytic ability.[79] Noble metal

Fig. 2 Polyaniline nanocomposite synthesis routes.

NPs are frequently used NPs in catalytic reduction processes because of their exceptional physicochemical traits and the presence of a wide number of binding sites due to the presence of bare atoms,[80,81] large surface area, and lower size.[82] However, noble metal catalysts exhibit low mass transport rate, unstable deactivation, and deficient catalyst use coefficient are other challenges that limit their application.[82] Thus, under numerous conditions, the use of metallic nanoparticles would stumble upon the aggregation of NPs owing to the higher surface energy in a smaller size,[83,84] poor separation and recovery from the reaction medium,[78] and lower stability and reusability, resulting in poor activity and complications in sustainable use. Numerous methods have been adopted and executed to overcome these limitations of pure metal-based nanoparticle catalysts, among which the immobilization of metal nanoparticles on the solid supporting surface has been considered an effective mechanism,[85–87] helping in the reduction of agglomeration of nanoparticles and isolation from the reaction medium. Embedding or immobilizing pure metal NPs into the polymer matrix may improve the reaction rate.[88] Various conducting polymers have been explored as supporting surfaces for immobilizing pure metal-based NPs, such as PPy and PANI. Among them, PANI is a widely studied and utilized conducting polymer as a supporting surface for immobilizing metal-based nanoparticles owing to its strong interaction with metal-based nanomaterials, and it has drawn vital interest in research due to the various effective immobilization of the metal NPs.[89]

Table 2 Synthesis procedure for the polyaniline nanocomposite

Preparation method	Description	Reference
In situ polymerization	Already fabricated nanomaterials are mixed in an acidic solution of aniline monomer. Next, polymerization is initiated by the drop-wise addition of an oxidant solution under constant stirring conditions, generating a nanocomposite with better dispersal of nanomaterials in the PANI matrix	60
Electrochemical polymerization	Pre-synthesized nanomaterial is dispersed in an aqueous/solvent solution of aniline that possesses a dopant, and the polymerization reaction of aniline is commenced by passing the current	61
Thermal reflux	Refluxing nanomaterial precursor and aniline in a suitable solvent at the apposite temperature generates PANI nanocomposite	62
Mixing	Physical mixing of pre-synthesized nanomaterial and PANI *via* milling, solution (in the same solvent or different solvents), or melt mixing	63
Sonochemical polymerization	Pre-synthesized nanomaterial is mixed in an aniline solution through ultrasonication and the polymerization reaction is initiated by adding of oxidizing agent	64
Chemical vapor deposition	Vapor phase polymerization of aniline monomers on the surface of a substrate that is coated with oxidant and nanocomposite obtained in the film form	65
Electrospinning	Formation of fibrous composite using a micro syringe pump by applying a voltage	66
Hydrothermal method	Formation of composite *via* hydrolysis at high temperature	67
Interfacial polymerization	Polymerization in a biphasic system, *i.e.* an aqueous/organic that splits the byproducts upon the basis of their solubility	68 and 69

Moreover, as a shell material, PANI has largely studied conducting polymer due to its distinctive electrical features, and the presence of effective anchoring sites for metal ion binding, which helps in the prevention of aggregation, easy synthesis, ecological stability, and biocompatibility, is another charismatic feature of PANI.[79,90,91] Since 1989, when the first report on the catalytic reduction of water pollutants was published,[92] various research groups reported numerous studies for the reduction of pollutants.[2,93] The key aimed water contaminants in the catalytic reduction studies are organic dyes (RhB, MO, CR, MG, EY, and MB), nitro- and nitroso-compounds (nitrophenols, trinitrotoluene, RDX, and NDMA), organic halides (bromi/chlori/fluorinated hydrocarbons), and hazardous oxyanions.[94] In the catalysis process, metal NPs lower the kinetic barrier for redox reactions and the decomposition of water pollutants.[95,96]

PANI in pure form with dopants can act as a catalyst due to its ease of conversion of benzenoid and quinoid rings in the PANI chain; however, its activity is comparatively low. PANI nanofibers are prepared using granite waste as an oxidant for the catalytic degradation of water pollutants, particularly 4-nitrophenol (4-NP) and Rhodamine B (RhB) dye, in the presence of NaBH$_4$. The reduction processes of 4-NP and RhB dye were completed in 40 and 5 min, with reaction rate constants of 0.0488 and 0.958 min^{-1}, respectively.[97] This reflects that pure PANI can act as a catalyst for the reduction of pollutants but suffers from poor activity.

PANI in comparison to conventional supporting materials for metal-based NPs is beneficial due to facile and inexpensive large-scale synthesis using oxidants, and the synthesis process can be made efficient using clean oxidizing agents, such as H$_2$O$_2$ and molecular O$_2$. Moreover, PANI properties can be modified by introducing various functionalities, making it a versatile support compared to inorganic materials. Using PANI as a supporting material for metal NPs, mainly noble metals (Au, Ag, Pd, and Pt), numerous composite catalysts have been produced and successfully explored for the degradation of various organic and inorganic chemical pollutants as well as biological water pollutants. Usually, the preparation of hybrids of noble metal NPs and conducting polymer can be achieved through in situ polymerization of monomer in the presence of metal NPs,[98–100] simultaneous reduction of metal ions, polymerization of aniline monomer with and/or without using oxidant,[101,102] direct blending of CP and metal NPs,[78,103,104] in situ reduction of noble metal ions by CP.,[97,105,106] one-pot synthesis of CP and noble metal NPs,[107] γ-radiolysis process in which the reaction mixture is exposed to γ-rays.,[108,109] interfacial polymerization in which a biphasic system i.e. an aqueous/organic phase splits the byproducts upon the basis of their solubility is utilized,[110] electropolymerization that proceeds by passing electric current in the reaction mixture of aniline and metal ion or NPs using solvent,[111,112] template-based synthesis process utilizing structure-guiding models to state the physical features of the resulting nanocomposite,[113] and self-assembly including physically mixing and/or grinding of PANI and metal NPs.[114]

PANI nanocomposites prepared via different methods using various nanomaterials, such as metal NPs, carbon materials, organic materials, and polymeric substances, are frequently utilized for the treatment of water in various ways, including heterogeneous catalytic degradation,[123] and other processes which include the photocatalytic degradation of pollutants using photocatalysts under light exposure,[124,125] adsorptive removal of pollutants using composites as adsorbent materials,[126–128] nano-filtration of pollutants using PANI-based materials as membranes,[129–131] sensing of pollutants using as sensors,[132–134] and disinfecting water from bio-organisms employing PANI composites as antimicrobial agents[135,136] (Fig. 3). Among them, the application of PANI nanocomposites as heterogeneous catalysts for the catalytic reduction of toxic water pollutants into less and/or non-toxic products has drawn immense attention. Using different types of metal-based nanomaterials, various PANI binary nanocomposites have been developed, as summarized in Table 3 and efficiently utilized as heterogeneous catalysts for the catalytic reduction of various water pollutants, such as nitroaromatics, organic dyes, pesticides, metal ions, and phenolic compounds.

The in situ polymerization process produces amorphous nanocomposite in which nanoparticles are homogeneously dispersed in a polymer matrix, but the unreacted reactant present with nanocomposite may affect its characteristics.[137] Through the in situ reduction process, the metal NPs are present at the surface of CP instead of embedded in the matrix; hence, they are available for direct interaction with the substrate, thus demonstrating good heterogeneous catalysis,[99,138] and the catalytic activity of the nanocomposite catalyst depends on the size of metal NPs.[106] Chen et al.[139] synthesized PANI/Pt hybrid nanocomposite catalyst via an in situ reduction process in which Pt^{6+} ions were reduced by citric acid doped PANI into small-size Pt NPs at the surface of PANI and dispersed uniformly, which exhibited excellent heterogeneous catalytic activity for the reduction of nitroaromatics, high reusability, and durability (Fig. 4). Through the direct blending process of CP and metal NPs, noble metal NPs can be deposited on the PANI surface of composites.[140]

To provide support to Au NPs, Sun et al.[84] reported Au NPs immobilized in PANI microtube (PANI/Au) composite via a template-free process that demonstrated effective catalysis of nitrophenols in the aqueous medium due to the higher surface area of microtubes and better dispersion, and the effective prevention of agglomeration of Au particles enhanced the stability and recovery potential of Au NPs (Fig. 5(a)). The nitrophenol reduction activity was observed in the order of 3-NP > 2-NP > 4-NP. A binary Au encapsulated (AuNP-PANI) water-soluble nanocatalyst was synthesized in a two-step process through the formation of micelle for stabilization of PANI NPs using surfactant CTAB, and the produced AuNP-PANI catalyst showed effective reduction for CR and MB dyes.[83] Similarly, a binary PANI/Au heterogeneous catalyst was prepared via interfacial polymerization using AuCl$_4^-$ as a source of Au NPs for the catalytic reduction of RhB dye. The AuCl$_4^-$ initiated the polymerization of aniline, and itself was reduced into Au NPs deposited on the surface of PANI.[142] Pd NP-loaded binary Pd@PANI catalyst with a very low amount of Pd NPs was produced via joint method interfacial polymerization and in situ
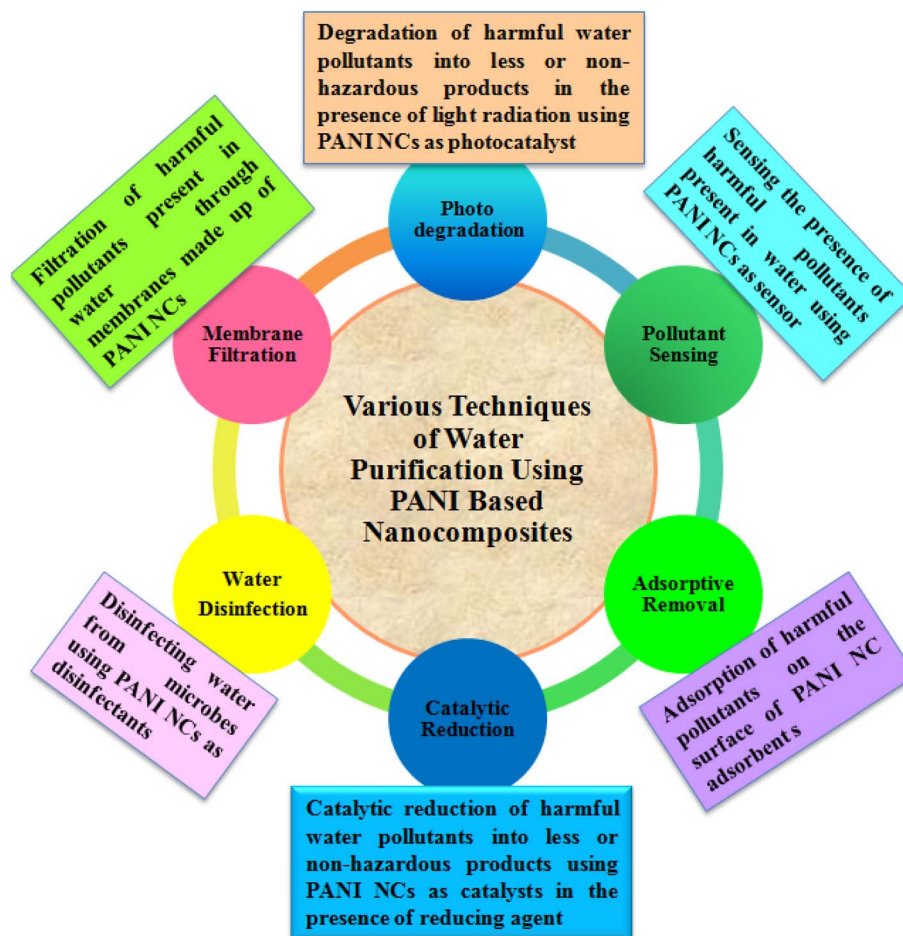
Fig. 3 Application of polyaniline-based nanocomposites in different water treatment procedures.

Table 3 PANI-based binary heterogeneous catalysts for catalytic reduction of pollutants[a]

PANI nanocomposite	Pollutant type	Catalyst dose	Rate constant	Time	References
PANI/Ni(0)	BG	0.025 g	0.113 min^{-1}	120 min	82
Au-PANI	MB	1 mg	33 × 10^{-2} s^{-1}	10 min	83
	CR	1 mg	30 × 10^{-2} s^{-1}	10 min	
PANI/Au	4-NP	0.0315 g	11.8 × 10^{-3} s^{-1}	270 s	84
	3-NP	0.0315 g	28.9 × 10^{-3} s^{-1}	90 s	
	2-NP	0.0315 g	22.3 × 10^{-3} s^{-1}	100 s	
PANI/Ag	4-NP	2.7 mg	21 × 10^{-3} s^{-1}	3 min	115
PANIsphere-Ag	4-NP	15.27	16 × 10^{-2} min^{-1}	23 min	116
PANI/Bi$_2$O$_3$	4-NP	0.1 g	—	15 min	117
Pd-PANI	4-NP	30 μL	20 × 10^{-3} s^{-1}	4 min	118
	MB		29 × 10^{-3} s^{-1}	2.5 min	
PANI/Ag	4-NP	—	9.5 × 10^{-3} s^{-1}	—	119
Pd/PANI	4-NP	30 mg	6.4 × 10^{-4} s^{-1}	40 min	120
PANI/Pt	4-NP	0.4 mol%	—	120 min	121
Ag-PANI	4-NP	1 mg	3.9 × 10^{-3} s^{-1}	300 s	122

[a] Catalyst dose amount (g = gram, μL = microlitre, mg = milligram, and mol% = mole percentage), reaction time (min = minute and s = second).

process using camphor sulfonic acid ((+)-CSA) as a dopant, and the obtained catalyst displayed effective reduction potential for nitroarenes in a water solution with a small quantity of reducing agent NaBH$_4$. The Pd@PANI catalyst exhibited good reusability and stability for numerous cyclic reuses, and the reused catalyst

demonstrated an improved catalytic rate (11.2 × 10^{-4} s^{-1}) compared to the fresh catalyst (6.4 × 10^{-4} s^{-1}).[120]

A phytic acid (PA) used as a dopant and crosslinker Ag NP-immobilized PANI nanocomposite recyclable (PANI/Ag) catalyst with a 3D structure was fabricated *via* an *in situ* redox
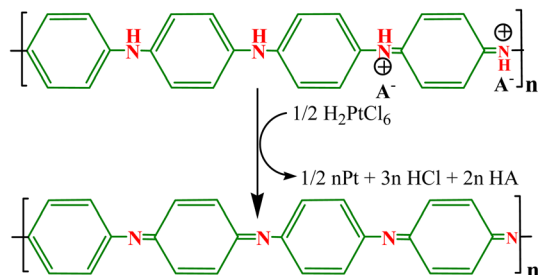
Fig. 4   Reduction of Pt^{6+} ions into Pt NPs.[139]

reaction between silver nitrate and PANI. The characteristic 3D porous structure of the prepared catalyst is formed by good dispersion of Ag NPs in the coral-shaped PANI, demonstrating remarkable catalytic performance toward 4-NP with a fast rate of reduction reaction (9.5×10^{-3} s^{-1}) due to constructive mass/electron transfer of the 3D porous structure and good attraction of Ag with PA; additionally, the magnetic features improve catalyst recyclability using an external magnetic field and retained high-level activity of up to six cyclic runs.[119] In another study, Chang et al.[115] prepared an Ag/PANI composite by depositing Ag NPs on the supporting surface of PANI achieved by in situ chemical reduction of AgNO$_3$ and further utilized for the catalytic reduction of 4-NP. The reduction of 4-NP occurred on the surface of Ag/PANI due to the stacking of 4-NP via π–π interactions with PANI, which is not possible with pure Ag NPs. Ni NPs are utilized as catalysts for the degradation of various pollutants owing to their eco-friendly nature, better electron-donating potential, excellent magnetic characteristics, and inexpensiveness. However, as a Fenton-type heterogeneous catalyst, Ni NP application is limited due to the lower stability and formation of aggregates. Various nanomaterials have been

successfully used as supporting materials for Ni(0) NPs, resulting in catalytic applications in numerous reactions. Bhaumik et al.[82] developed Ni(0) metal NPs supported on a nanotubular porous PANI matrix (PANI/Ni^0 NCs) nanocomposite catalyst (illustrated in Fig. 5(b) (SEM image) and Fig. 5(c) (TEM image)) via a reductive formation process that exhibited Fenton-like catalytic activity for the BG dye in water samples in the presence of H$_2$O$_2$. The PANI/Ni^0 NC catalyst exhibited supremacy compared to pristine Ni^0 NPs for BG degradation and degraded 100% of the BG dye within 120 min. Moreover, it retained its activity (100%) in five cyclic experiments.

Ultrafine Pt NPs immobilized on surfaces of PANI nanofibers catalyst (PANI/Pt) were fabricated via a facile solution procedure. The Pt NPs were deposited on PANI fibers via an in situ reduction process, and the catalyst illustrated greater activity against nitrobenzene and showed excellent stability, reusability, and durability.[139] Ag NPs loaded on citric-acid (CA)-modified PANI catalyst (Ag@PCA) were produced through an in situ reduction process and utilized for the reduction of nitrophenols. The obtained electrocatalyst showed effective activity for the oxidization of 2-NP and 4-NP.[143] Pd NPs immobilized PANI (Pd-PANI) catalyst prepared using surfactant-based liquid crystalline mesophase by employing chemical oxidation, followed by in situ radiolytic reduction of Pd^{2+} ions on the PANI nanowire surfaces. The developed catalyst demonstrated good reduction potential against 4-NP and MB dye due to the effective immobilization of Pd NPs and homogenous dispersion and showed better stability.[118] Metal oxides, such as CuO[144] and Bi$_2$O$_3$,[145,146] alone have been explored for the catalytic degradation of numerous water pollutants. Recently, green synthesized CuO NPs utilized for the reduction of 4-NP[144] and biogenic pure Bi$_2$O$_3$ (ref. 145 and 146) demonstrated effective catalytic ability
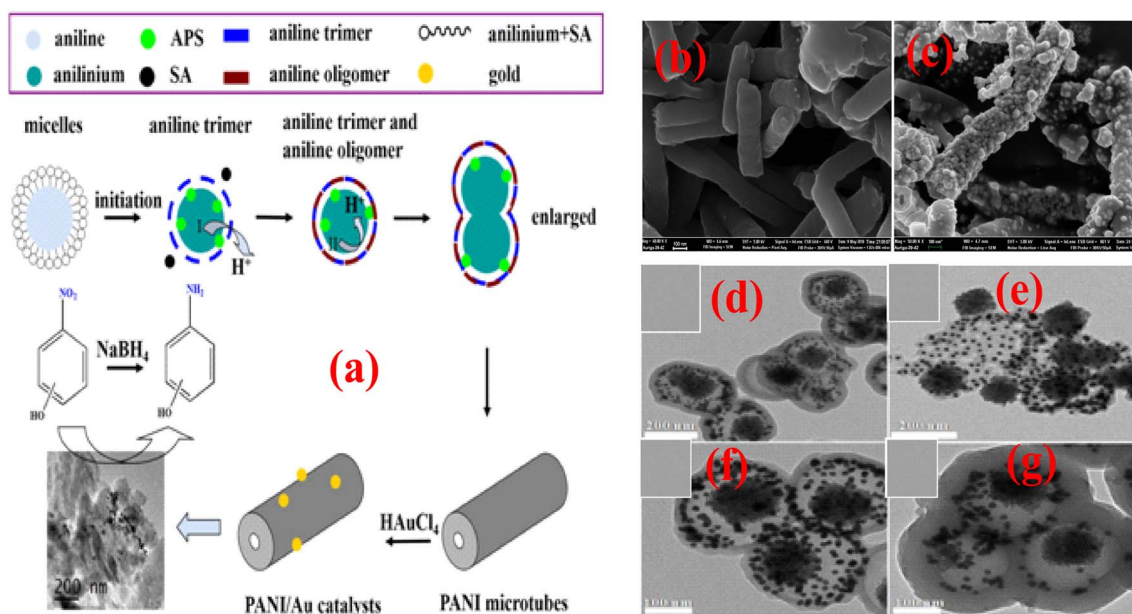

Fig. 5   (a) Synthesis scheme for PANI microtubes and the PANI/Au catalyst,[84] (b) SEM and (c) TEM image of PANI/Ni^0 NCs,[82] and (d–g) TEM images of the Fe$_3$O$_4$@Au-PANI ternary nanocomposite.[141]

for nitroaromatics and organic dyes, similar to Ag_2O in pristine form or as a composite utilized for catalytic reduction of nitroaromatics and dye pollutants.[147] However, in pure form, metal oxide NPs demonstrate relatively poor activity, recovery, reusability, and stability. By providing support or immobilizing with polymeric materials, especially PANI polymers, the activity of metal oxide NPs can be enhanced. For instance, immobilization of Bi_2O_3 NPs in PANI (PANI/Bi_2O_3) significantly empowered the reduction ability of Bi_2O_3 for 4-NP in an aqueous medium and reduced about 95.4% of 4-NP within a short time (10 min) by a small amount of catalyst (0.1 g) and also enhanced the stability of Bi_2O_3 particles.[117]

However, the application of PANI as a support material suffers from recovery and reuse issues.[93] This limitation can be overcome by introducing magnetic characteristics to the PANI-supported metal-based NPs, which can be easily and effectively isolated and recovered by applying an external magnet. Producing magnetic characteristics in the nanoparticles by supporting magnetic materials prevents particle aggregation and causes ease of isolation and revival from the reaction solution by applying an external magnetic field.[78] However, in an acid solution, the magnetic material particles exhibit poor stability and may react with catalyst(s) to be immobilized or even with the substrate; thus, their surface should be covered by forming a core–shell composite structure in which the shell can effectively protect the magnetic core particles. For the shielding of the magnetic core, numerous materials, such as carbon, silica, TiO_2, other inorganic materials, and polymers, are widely utilized and have successfully helped in the prevention of corrosion, enhanced interaction, and improved inertness and stability. However, the use of polymeric shells enhances stability and magnifies the biocompatibility and solubility of magnetic material particles in water.[78,148] PANI is one of the most widely studied and employed polymer materials as a shell for magnetic and other cores.[78]

In recent years, extensive research has been carried out on the development of magnetic and nonmagnetic PANI-supported metal-based ternary and quaternary nanocomposite catalysts for water treatment. A few of them that have been successfully employed for the catalytic degradation of various pollutants are listed in Table 4. For example, bifunctional Au immobilized $Fe_3O_4@C$ ($Fe_3O_4@C@Au$) composite microspheres developed by coating Au NPs on the surface of functionalized $Fe_3O_4@C$ microspheres showed excellent degradation ability for MB dye due to synergistic effects of small particles of Au NPs, excellent adsorption tendency of C-layers and better dispersion of the microspheres. The $Fe_3O_4@C@Au$ catalyst degraded MB dye with a reaction rate of 0.331 min^{-1}.[160] Chen et al.[78] protected the magnetic core using a PANI polymer shell and prepared $Fe_3O_4@PANI$ core–shell nanostructure via an in situ polymerization process, which was utilized as solid support for Au nanoparticles to produce $Fe_3O_4@PANI@Au$ composite catalyst. The Au NPs were adsorbed on the PANI surface via electrostatic interactions. The magnetic core shell-supported Au-based composite catalyst prepared in this way was utilized for the reduction of CR dye using $NaBH_4$ as a reducing agent. After completion of the reaction, the utilized catalyst was separated

and recovered effectively via an external magnetic field. Within 6 min of reaction time, the CR dye was reduced by 10 mg of catalyst, and it demonstrated good activity for up to five cyclic uses without losing significant activity. Ternary magnetic PANI-supported Ag ($MnFe_2O_4@PANI@Ag$) nanocatalyst synthesized via a simple reflux process demonstrated good activity for the degradation of organic dyes MO, EY, MB, and RhB in the presence of $NaBH_4$; converted into colorless non-toxic forms quickly within 9, 16, 7, and 23 min, respectively; easily recovered via magnetic separation and exhibited good activity up to four cycles of reuses. The magnetic core and PANI fibrous linker shell effectively stabilized Ag particles with good dispersion and minimum aggregation.[149] Zhang et al.[103] used cobalt spinel ($CoFe_2O_4$) as a magnetic core material to produce ternary core shell $CoFe_2O_4/PANI/Au$ nanocomposite catalyst for the catalytic reduction of 4-NP, which demonstrated excellent catalytic reactivity (100% reduction after 8 min) in a short time, and good recovery and stability.[103]

Zhu et al.[150] synthesized core–shell magnetic $Fe_3O_4@$-$PANI@Au$ nanocomposite catalyst via electrostatic self-assembly and seed growth processes that exhibited good reduction potential for organic pollutants (4-NP, MO, MB, and RhB) and inorganic pollutant (Cr(VI)) in an aqueous medium and demonstrated good stability, recovery, and reusability. Via controllable coating of PANI, Jin et al.[151] prepared a magnetic ternary $Au@Fe_3O_4@PANI$ nanocomposite catalyst for the catalytic reduction of 4-NP using $NaBH_4$ as the reducing agent. The presence of PANI and iron oxide showed good stability and recyclability and improved the catalytic performance of Au NPs owing to their synergetic effects. The catalyst reduced 4-NP with a high rate of reaction and demonstrated excellent reusability of up to 10 cycles. Moreover, $Fe_3O_4@PANI@Au$ exhibited good selectivity toward the degradation of cationic dyes and rapidly degraded CR dye. Bioinspired reduction of Au^{3+} ions using plant Allium sp. extract at the surface of magnetic core–shell $Fe_3O_4@PANI$ nanocomposite generated $Fe_3O_4@PANI$-Au catalyst for reduction of hazardous dyes MB and MO using reducing agent. With a small amount of biosynthesized catalyst (1 mg and 2 mg), the dyes were reduced in a very short time. In the presence of 1 mg of catalyst dose, the MB and MO dyes took 50 and 60 s, respectively, while with 2 mg of catalyst dose, they decolorized in 60 and 80 s, respectively. The catalyst retained its activity for a long time (up to 8 cyclic reuses) and displayed good stability.[152]

Core–shell composite structures that possess a movable core inside a hollow capsule represent yolk–shell structures; they are extensions of conventional core shell structures.[142,161] In comparison to traditional core shell structures, empty parts of yolk–shell structures possess a higher unoccupied space, low density, and a greater surface area. Various types of yolk–shell composites composed of a magnetic core and a functional shell have drawn wide attention as catalyst-supporting structures. The outer shell of yolk–shell type composite structures demonstrating greater surface area and effective dispersion features enables them to provide better support to the catalyst and maximize their catalytic potential to metal NPs.

Table 4 PANI-based ternary and quaternary heterogeneous catalysts for catalytic reduction of pollutants[a]

PANI nanocomposite	Pollutant type	Catalyst dose	Rate constant	Time	References
AgCl/PANI/D-Dex	4-NP	10 mg	0.365 min^{-1}	6 min	69
Fe$_3$O$_4$@PANI@Au	CR	10 mg	0.80 min^{-1}	6 min	78
Au-PANI@mGO	4-NP	10 mg	86.3×10^{-2} min^{-1}	5 min	93
	CR	10 mg	28.64×10^{-2} min^{-1}	20 min	
	MB	10 mg	68.19×10^{-2} min^{-1}	5 min	
	RhB	10 mg	94.02×10^{-2} min^{-1}	4 min	
Fe$_3$O$_4$@PANI/Ni@Pd	O-NA	1 mg mL^{-1}	—	3 min	97
Fe$_3$O$_4$@PANI/Au/m-SiO$_2$	4-NP	0.9 mL	25.49×10^{-3} min^{-1}	40 min	99
PS/PANI@Au	4-NP	0.375 mL	36×10^{-3} s^{-1}	—	104
Ag-PANI-MWCNT	4-NP	1 mg	5.4×10^{-3} s^{-1}	240 s	122
PANI/ZnO/MnO$_2$	4-NP	10 mg	21.9×10^{-2} min^{-1}	10 min	123
rGO-PANI/Pd:Au	4-NP	2 mg	5.8×10^{-3} s^{-1}	8 min	136
	O-NA	2 mg	5.4×10^{-3} s^{-1}	8 min	
	RhB	2 mg	7.3×10^{-3} s^{-1}	30 min	
	MG	2 mg	9.5×10^{-3} s^{-1}	30 min	
	Cr(VI)	2 mg	—	30 min	
PS/PANI-Au	4-NP	0.12 mL	9.5×10^{-3} s^{-1}	13 min	140
MnFe$_2$O$_4$@PANI@Ag	MB	1 mg	61×10^{-2} min^{-1}	7 min	149
	MO	1 mg	22×10^{-2} min^{-1}	9 min	
	EY	1 mg	14×10^{-2} min^{-1}	16 min	
	RhB	1 mg	11×10^{-2} min^{-1}	11 min	
Fe$_3$O$_4$@PANI@Au	4-NP	20 ug	8.63×10^{-3} s^{-1}	210 s	150
	CR	20 ug	11.91×10^{-3} s^{-1}	90 s	
	MO	20 ug	16.11×10^{-3} s^{-1}	90 s	
	MB	20 ug	10.59×10^{-3} s^{-1}	150 s	
	RhB	20 ug	6.41×10^{-3} s^{-1}	240 s	
Au@Fe$_3$O$_4$@PANI	4-NP	25 uL	43.3×10^{-2} min^{-1}	5 min	151
Fe$_3$O$_4$@PANI-Au	MO	1 mg	2.21×10^{-2} s^{-1}	60 s	152
	MB	1 mg	3.17×10^{-2} s^{-1}	80 s	
Fe$_3$O$_4$@Au-PANI	4-NP	3 mg mL^{-1}	12.4×10^{-2} min^{-1}	28 min	141
Cu(0)-PANI-ZrSiO$_4$	4-NP	1 mg	81.1×10^{-2} min^{-1}	10 min	153
	3-NP	1 mg	24.9×10^{-2} min^{-1}	7 min	
	2-NP	1 mg	58.4×10^{-2} min^{-1}	5 min	
PANI/MnO$_2$/TiO$_2$	Cr(VI)	1 mg mL^{-1}	15.97×10^{-2} min^{-1}	5 min	154
PS/PANI/Au	4-NP	—	58.66×10^{-3} s^{-1}	60 s	155
Ag$_3$PO$_4$/Ppy/PANI	4-NP	—	5.3×10^{-3} min^{-1}	—	156
Ni(OH)$_2$@NSA-PANI	4-NP	5 mg	82.98×10^{-3} min^{-1}	24 min	157
Ag@PANI–CS–Fe$_3$O$_4$	4-NP	1 mg	2×10^{-3} s^{-1}	22 min	158
Pd@PANI–CS–Fe$_3$O$_4$	4-NP	1 mg	5.0×10^{-3} s^{-1}	22 min	159

[a] Catalyst dose amount (mg = milligram; ug = microgram), reaction time (min = minute; s = second).

Qiao et al.[141] reported a yolk–shell type ternary composite Fe$_3$O$_4$@Au-PANI catalyst (TEM images shown in Fig. 5(d–g)) in which Au NPs were immobilized in a PANI shell that has a magnetic core via a SiO$_2$ sacrificial template procedure. The Au NPs were anchored onto the inner layer of the PANI shell to avoid direct interaction with the substrate molecules. Thus, the presence of a magnetic core allowed facile recovery of the catalyst, and the PANI supported and protected the catalyst from an outer atmosphere. The catalyst with a PANI protection shell (Fe$_3$O$_4$@Au-PANI) demonstrated higher reduction potential against 4-NP than the catalyst without a PANI shell. The multistep synthesis procedure used to prepare Ni@Pd core–shell NPs was immobilized on magnetic Fe$_3$O$_4$@PANI yolk–shell nanocomposite. The yolk–shell was prepared via ultrasound-mediated in situ polymerization of aniline on Fe$_3$O$_4$@SiO$_2$. Then, the silica layer was etched selectively to obtain a yolk–shell structure. Finally, the Ni@Pd core was inserted by

dispersion in an aqueous medium with a reducing agent and metal precursors. The catalytic performance of the prepared yolk–shell quaternary Fe$_3$O$_4$@PANI/Ni@Pd catalyst was investigated against o-nitroaniline, which reduced by 99% in 3 min.[79]

Magnetic materials suffer from aggregation issues, which can be prevented by carbon-based materials. Recently, the use of carbon materials (GO, rGO) as support for metal NPs to produce heterogeneous catalysts can effectively prevent the aggregation of particles, facilitate dispersion in an aqueous medium, enhance the accessibility of the catalyst to pollutants, and improve the surface area and electron transfer process efficiently. By following multiphase, Pourjavadi et al.[93] produced Au NPs supported on magnetic PANI@mGO composite catalyst that showed remarkable reduction ability for CR, RhB, MB, and 4-NP in aqueous phase due to good dispersion ability; higher surface area due to the presence of GO; and facile electron transfer during catalysis process due to better attraction with

PANI, and also displayed good recoverability on applying an external magnetic field.[79] In nonmagnetic PANI-based ternary nanocomposite, the PANI provided better support surface to metal-based NPs and was exploited for catalytic degradation of water pollutants. Ternary composite containing polystyrene core and PANI shell, such as PS/PANI/Au catalyst, developed by Sun et al.[155] using sulfonated polystyrene, Au(en)$_2$Cl$_3$, and aniline for the degradation of 4-NP that completely reduced 4-NP into 4-AP within a very short time (60 s). Similarly, a heterogeneous catalyst PS/PANI@Au developed via the seed swelling polymerization process and in situ reduction method was employed for the effective reduction of toxic pollutant 4-NP. In the prepared catalyst, PS survived as the core and template, and the shell was formed by PANI and Au NPs. Moreover, the dedoping of the PS/PANI@Au catalyst was carried out using acid and showed a higher reduction performance for 4-NP than that of the doped catalyst.[104]

Through the direct blending of core–shell PS/PANI binary composites and metal NPs produced from noble metals NPs (Au, Ag, Pd, Pt) deposited on PANI shell surface due to attraction between positive surface of PANI and negative charge on metal NPs under weak acidic medium through simple electrostatic self-assembly process, the produced PS/PANi-MNPs composite represented raspberry-like morphology (Fig. 6 SEM images). The PS/PANi-Au nanocomposite catalysts were prepared in three types using three sizes (32.4, 17.5, and 3.1 nm) of Au NPs and applied for the reduction of 4-NP, which reduced it with reduction rates of 3.8×10^{-3}, 7.0×10^{-3}, and 1.3×10^{-2} s^{-1}, respectively. The results of the reaction indicated that the reaction rate decreases as the particle size of Au NPs increases in the PS/PANi-Au nanocomposite catalyst. This is because the

reduction reaction of 4-NP chiefly progresses on the surface of Au NPs, and smaller-size NPs (Au) possess greater reduction ability owing to the enhanced density of active edges and corner sites at the surface of Au NPs.[140] Sun et al.[162] utilized a copolymerization process for the synthesis of a (P(ANI-co-Py)) copolymer and produced Au NP-immobilized (P(ANI-co-Py)) composite catalyst by deposition of Au NPs using a sol–gel process. Similarly, binary Au/PANI and Au/PPy were also synthesized. The copolymer effectively stabilized small Au NPs and enhanced the catalytic activity of 4-NP. Due to the good dispersion of Au NPs in the support material, the strong interaction of metal-support and the effective adsorption of 4-NP on the catalyst surface owing to the negative surface of Au NPs increased the catalytic ability of the prepared catalyst.

Recently, a core–shell type ternary catalyst in which a CNT-supported Pt (Pt/CNT) core was covered with a PANI shell to obtain Pt/CNT@PANI catalyst for the catalytic hydrogenation of Cr(VI). The Pt NPs completely wrapped with PANI exhibited excellent reduction performance against Cr(VI) in a liquid medium because of the redox characteristics of PANI, in which initially the Cr(VI) oxidized PANI and itself turned into Cr(III), followed by the catalytic hydrogenation in which PANI (oxidized) again transformed into PANI (reduced). A reusability of 92.4 was reported after the fourth catalytic recycle, which indicated good stability of the Pt/CNT@PANI.[163] PANI-supported ternary metal oxide in which one of the components is MnO$_2$ demonstrated good catalytic reduction ability against organic and inorganic water pollutants because Mn^{4+} can oxidize and reduce into higher and lower oxidation states. PANI-supported metal oxide ternary nanocomposites containing MnO$_2$ as one component were synthesized and employed
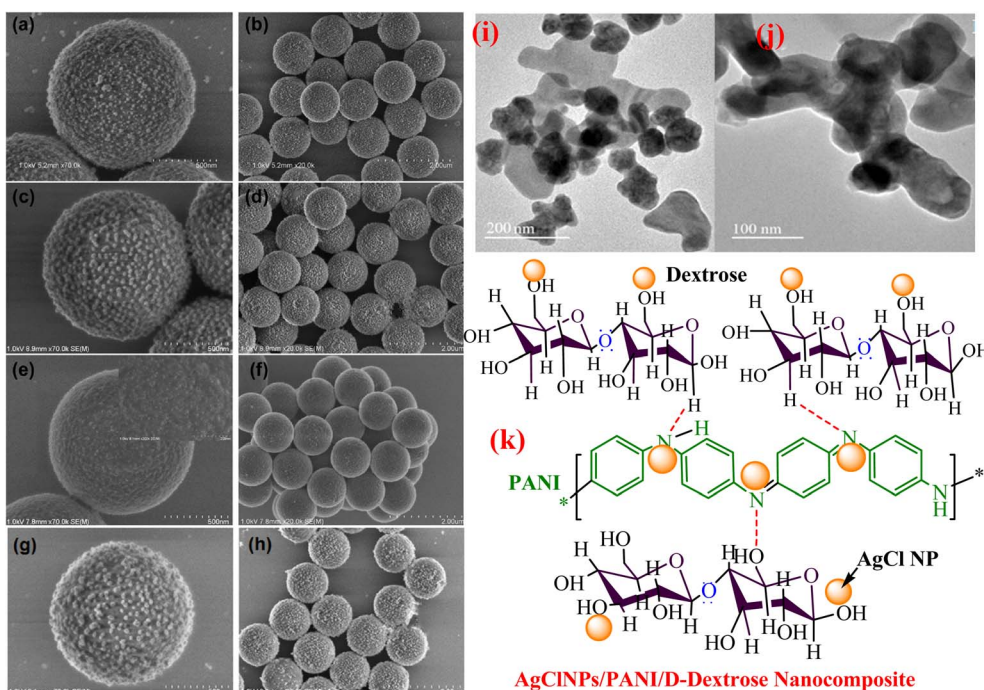

Fig. 6 (a and b) PS/PANi-Ag, (c and d) PS/PANi-Pt, (e and f) PS/PANi-Pd, (g and h) PS/PANi-Au composite SEM images,[140] (i and j) HR-TEM images of the PANI/MnO$_2$/TiO$_2$ nanocomposite,[154] and (k) structure of AgClNPs/PANI/D-Dex.[69]

for the reductive degradation of pollutants.[123,154] PANI/ZnO/MnO$_2$ catalyst prepared by Meena and Saini[123] *via* a three-step process and utilized for the catalytic degradation of 4-NP demonstrated a good catalytic reduction in an aqueous medium in a short time (10 min) due to a synergistic relationship and better stability. In another study, MnO$_2$ containing PANI-supported ternary nanocomposite PANI/MnO$_2$/TiO$_2$ catalyst (Fig. 6(i and j) HRTEM images) was utilized for the catalytic reduction of toxic Cr(VI) ions.[154] The composite was produced by employing a one-pot redox polymerization process at ambient temperature. In comparison to binary (PANI/MnO$_2$, MnO$_2$/TiO$_2$, PANI/TiO$_2$) and bare (MnO$_2$, TiO$_2$, PANI), the ternary composite effectively (99.9%) reduced Cr(VI) to Cr(III) in the presence of HCOOH.

Ma and co-workers[156] tested a PANI-based ternary nanocomposite Ag$_3$PO$_4$/PPy/PANI as a heterogeneous catalyst for the catalytic reduction of 4-NP and 2-NA using reducing agent NaBH$_4$ and reported that the as-prepared Ag$_3$PO$_4$/PPy/PANI can be used as a potential catalyst for the reductive degradation of water pollutants. Ag NP-supported PANI/MWCNT ternary composite catalyst obtained by the immobilization of Ag NPs on the PANI surface and then added with the MWCNTs showed excellent reduction ability against 4-NP with 0.054 s^{-1} of rate constant and good antibacterial activity towards pathogenic bacteria, which revealed many uses of Ag NPs-PANI/MWCNTs and showed a wide scope of applications in the healthcare and environmental segments.[122] Copper metal NP-based ternary composite catalyst Cu^0-PANI-ZrSiO$_4$ synthesized *via* surface immobilization of Cu(0) NPs on the nanozirconium silicate modified-PANI surface in a solvent-less microwave preparation process and applied for the reduction of various nitrophenols using NaBH$_4$ as a reducing agent that effectively reduced 4-NP, 3-NP, and 2-NP nitrophenols with the reduction rate of 0.811, 0.249, and 0.584 min^{-1}, respectively at pH = 2.[153]

Prabakaran and Pilla[69] integrated AgCl NPs into a PANI-grafted D-dextrose composite *via* an interfacial polymerization process, and synthesized AgClNPs/PANI/D-Dex (Fig. 6(k)) was applied for the degradation of 4-NP using NaBH$_4$ a reducing agent that displayed remarkable activity and decolorized yellow color of 4-NP in a short time due to reduction into 4-AP. During the degradation process of 4-NP by AgClNP/PANI/D-Dex nanocomposite catalyst, the 4-NP molecules and reducing agent ions were adsorbed on the active center of the catalyst AgCl NPs, which acted as an electron transferring surface. Pd NPs anchored on PANI were supported on mesoporous SBA-15 catalyst (Pd-NPs/PANI/SBA-15) fabricated *via* an *in situ* chemical process for catalytic reduction of BrO$_3^-$ ions. In the catalyst, the Pd NPs were efficiently immobilized on the amino functional groups of the PANI skeleton. The reduction of BrO$_3^-$ ion was analyzed *via* an electrochemical process, and during the reduction process, BrO$_3^-$ ions were diffused from the solution to active sites of Pd NPs, where they were catalytically reduced.[164] Ni(OH)$_2$ NPs decorated 2-NSA-doped PANI nanotube (Ni(OH)$_2$@NSA-PANI) nanocomposites (Fig. 7) used for the catalytic reduction of nitroaromatics. The catalyst was prepared by immobilized Ni(OH)$_2$ NPs on the surface of 2-NSA-doped PANI nanotubes. The catalyst effectively degraded (94%) 4-NP
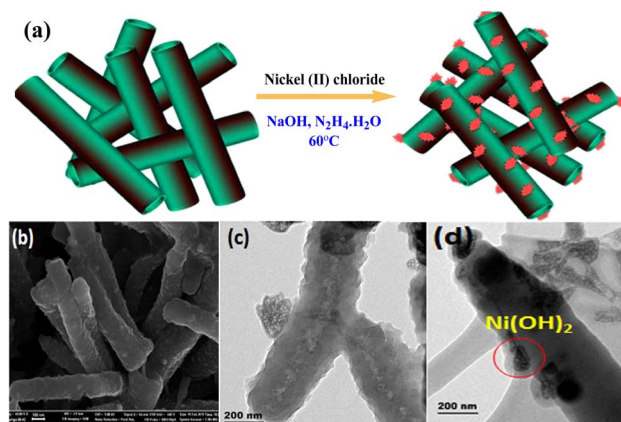

Fig. 7 (a) Synthesis process, (b) SEM image, (c) HR-TEM image and (d) STEM image in the dark field of Ni(OH)$_2$@NSA-PANI NCs.[157]

with a small amount of catalyst and showed recyclability without declining ability over ten repeating cycles. Ni(OH)$_2$ NPs present in the (Ni(OH)$_2$@NSA-PANI) nanocomposites acted as a reducing surface for the pollutant, and the pollutant ions along with BH$_4^-$ were adsorbed on Ni(OH)$_2$ NPs, which was the electron relay center for the reduction process.[157]

Al-saida and coauthors[165] reported the synthesis of four component quaternary magnetic core–shell type Fe$_3$O$_4$@TiO$_2$-PANI-Ag nanocomposite catalyst *via* the polymerization reaction of aniline onto magnetic core–shell structure Fe$_3$O$_4$@TiO$_2$ by APS as an oxidant and then attaching Ag NPs to it. The as-prepared Fe$_3$O$_4$@TiO$_2$-PANI-Ag catalyst was used in the reduction process of 4-NP and MB dye water pollutants. Moreover, >98% catalytic reduction of 4-NP was completed within 20 min when 1 mg of Fe$_3$O$_4$@TiO$_2$-PANI-Ag catalyst was utilized. Besides, it is reported that the Fe$_3$O$_4$@TiO$_2$-PANI-Ag catalyst showed higher competence than that of the binary PANI-Ag, TiO$_2$–Ag, and TiO$_2$/PANI composites due to the synergistic effect of PANI and Ag with TiO$_2$ shell, providing effective support to Ag NPs by PANI and effectively stabilizing them. Additionally, due to magnetic characteristics, the catalyst showed good recovery and reusability. With 2 and 3 mg of composite catalysts within 12 and 6 min of reaction time, the reduction of 4-NP was achieved due to the increase in the density of binding sites of the catalyst. The reduction time was reduced with an increase in the catalyst dose amount.[165]

Ayad *et al.*[158,159] in their studies reported the synthesis of quaternary composite catalysts of noble metal Pd and Ag NPs by encasing properties of conducting polymer PANI, biopolymer CS, and magnetic material Fe$_3$O$_4$. PANI and CS polymeric materials were utilized as supporting surfaces for noble metal (Pd and Ag) NPs, while magnetic Fe$_3$O$_4$ enhanced the isolation and recovery of the catalysts. The catalyst obtained in a multi-step procedure with magnetic features and effective functionalities (hydroxyl and amino) present with CS and PANI effectively coordinated with Pd and Ag ions and enabled their reduction and deposition. Thus, the quaternary Pd@PANI–CS–Fe$_3$O$_4$ (ref. 158) and Ag@PANI–CS–Fe$_3$O$_4$ (ref. 159) nanocomposite catalysts were fabricated *via* reductive deposition of

Pd and Ag NPs, respectively, on the surface of a ternary (PANI–CS–Fe$_3$O$_4$) composite utilized for the catalytic degradation of 4-NP, which showed good reduction potential. Pd@PANI–CS–Fe$_3$O$_4$ catalyst reduced 4-NP within 14 and 8 min of reaction times using 2 mg and 3 mg of catalysts, respectively, while Ag@PANI–CS–Fe$_3$O$_4$ catalyst took 22, 8, and 6 min with 1, 2, and 3 mg of catalysts, respectively.[159]

In comparison to mono metals, the bimetallic NPs exhibit higher catalytic potential and better permanence.[79,136] In this regard, rGO-PANI supported bimetallic (palladium (Pd): gold (Au)) NP composite catalysts developed for the catalytic degradation of numerous organic (RhB, MG, 4-NP, 4-NA) and inorganic (Cr(VI)) water pollutants, which showed improved catalytic ability compared to mono metallic NPs due to better electrostatic attractions between PANI, rGO and (Pd: Au) NPs *via* a synergistic effect.[136] In another study, a bimetallic quaternary yolk shell type Fe$_3$O$_4$@PANI/Ni@Pd composite synthesis was reported for the reduction of *o*-nitroaniline (*O*-NA) using NaBH$_4$ as a reducing agent and converted 99% of *O*-NA within 3 min. Initially, using a solvothermal process, Fe$_3$O$_4$ NPs were prepared, followed by coating the SiO$_2$ shell on the surface of Fe$_3$O$_4$ through the sol–gel process. Then, the PANI layer was introduced by ultrasound-mediated *in situ* polymerization of aniline and by selective etching of SiO$_2$ layer generated yolk–shell Fe$_3$O$_4$@PANI composite. The Ni@Pd NPs were immobilized on the yolk–shell Fe$_3$O$_4$@PANI composite by reduction of Pd^{2+} and Ni^{2+} salts using NaBH$_4$. The prepared Fe$_3$O$_4$@PANI/Ni@Pd exhibited a good conversion efficiency for *O*-NA for up to eight cycles, demonstrating good stability and reusability.[79]

Magnetic Fe$_3$O$_4$/PANI/*m*-SiO$_2$ core/shell spheres were used for the support of Au NPs to prepare highly stable, reusable, robust, and reactive quaternary composite catalyst Fe$_3$O$_4$/PANI/Au/*m*-SiO$_2$. The Au^{3+} ions were anchored on ternary Fe$_3$O$_4$/PANI/*m*-SiO$_2$ core/shell spheres *via* a reduction reaction that occurred between the metal ions and PANI. The magnetic core and mesoporous *m*-SiO$_2$ shell appreciably advanced the recycling competence and deeply strengthened the stability of Au metal NPs against aggregation, and PANI provided better attraction and reduced Au^{3+} ions. The presence of an *m*-SiO$_2$ shell reduces agglomeration and modifies the stability remarkably because it acted as a barrier against the nucleation of NPs and also worked as a conduit in the mass transfer process of reagents. The Fe$_3$O$_4$/PANI/Au/*m*-SiO$_2$ showed better activity and stability in the liquid phase, which designated its potential uses as competent heterogeneous catalysts in liquid-phase catalytic reactions. The reduction ability was tested with nitrophenols (4-NP, 3-NP, and 2-NP) and nitroanilines (4-NA, 3-NA, and 2-NA), which were degraded by the order of 4-NP > 2-NP > 3-NP and 4-NA > 2-NA > 3-NA, respectively.[99]

5. Mechanisms of catalytic reduction of water pollutants in the presence of PANI-based catalysts

PANI nanocomposites have been successfully explored as heterogeneous catalysts for the reductive elimination of numerous water pollutants, such as nitroaromatics (nitrophenols and nitroaniline), organic dyes, and oxyanions. Usually, the reduction of nitroaromatics into the corresponding amino products is kinetically restricted under normal conditions using a reducing agent such as NaBH$_4$ (ref. 102); this barrier cannot be crushed alone by a reducing agent only. Moreover, catalysts alone cannot change nitro compounds into aminophenol products. Thus, it is essential to break down this kinetic barrier that provides a surface for electron reliance, which is possible by adding a catalyst. Thus, the reduction of nitroaromatics and other pollutants occurs on the surface of the utilized catalyst, and the resulting product is desorbed from the surface and discharged in solution. Hence, for the effective catalytic reduction of pollutants, the presence of a suitable catalyst and reducing agent is needed, making the reduction process thermodynamically and kinetically favorable. During reduction reactions, the reducing agent (BH$_4^-$) works as an electron donor, while pollutant molecules work as an electron-acceptor centre.[166]
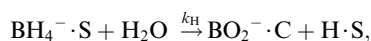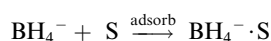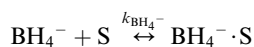
4-NP is a highly toxic nitrophenol that has severe health problems and environmental issues because of its lethal and mutagenic ability in living creatures, including humans.[167] The major health impacts of 4-NP are on the central nervous system (CNS), liver, and blood.[168] The catalytic reduction of the nitroaromatics into amino products is a significant industrial reaction; amines are the starting materials for numerous synthetic procedures to generate various dyes, pharmaceuticals, agrochemicals, and polymers.[169] Moreover, amino-products are moderately less hazardous, can be eliminated more easily, and are more mineralized than those of the nitroaromatics.[170] Nevertheless, the catalytic reductions of nitroaromatics, including 4-NP, occur at high-temperature conditions, take longer times and prominently use expensive catalysts. Recently, the use of polyaniline-based catalysts in the catalytic reduction process of 4-NP has gained wide interest.

The heterogeneous catalytic reduction process can precede either the L–H (Langmuir–Hinshelwood) or the E–R (Eley–Rideal mechanism). The L–H mechanism proceeds first to adsorb both the reducing agent (BH$_4^-$) and reactant (nitroaromatics, dyes) on the catalyst surface; then, the reaction is performed. According to the E–R mechanism, adsorption of one reactant molecule occurs, which reacts with the molecules of another reactant. Additionally, in the L–H pathway, with an increase in pollutant (nitroaromatics, dyes) value, the value of the apparent rate constant (k_{app}) decreases as the NaBH$_4$ concentration increases. However, in the E–R mechanism, the value of k_{app} enhances as the 4-NP amount enhances.[171] In the literature, it has been reported that the Langmuir–Hinshelwood (L–H) reaction mechanism model is widely followed for the catalytic reduction of nitrophenols and other dye pollutants. In addition to reducing agent NaBH$_4$ and catalyst to the reaction medium, the NaBH$_4$ produced Na$^+$ and BH$_4^-$ ions, and the produced BH$_4^-$ ions were adsorbed on the catalyst surface along with pollutant molecules and bound with the active part of catalysts, such as noble metal NPs, metal oxides or hydroxide or chloride NPs, and donated electrons to the active centre. After that, H$_2$ is produced by the reduction of water; then, active

hydrogen is generated at the surface of the catalyst.[69,172] The generated H_2 gas helps in stirring the reaction mixture, enhances the reaction rate, reduces reaction time, and refreshes the catalyst by removing any layer formed by oxide or other impurities on the NP surface by hydrogen flux.[166] In this way, due to the transfer of electrons from a donor (reducing agent) to an acceptor (reactant) *via* the catalyst surface, which acts as a relay centre, and the transfer of the required hydrogen atoms from the catalyst surface to the reactant, the reactant transforms it into its reduced state at the NP catalyst surface. The reduction of 4-NP into 4-AP occurs *via* the formation of a stable intermediate 4-hydroxyaminophenol, and the produced 4-AP molecules discharged from the catalyst surface provide a free catalyst surface and enter into the next catalytic cycle (Fig. 8). Hydrogen generation by the reduction of water molecules occurs as follows:

$$NaBH_4 + 2H_2O \rightarrow NaBO_2 + 4H_2$$
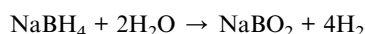
It is assumed that the adsorption of pollutants and borohydride on the NP surface is reversible and rapid. Additionally, the transformation reaction at the NP surface is slow and a rate-determining stage, and the desorption of the product from the catalyst surface is tacit to be speedy and irreversible; thus, it does not influence the kinetics of the reduction process.[173] It is well established from studies that the reduction reactions of nitroaromatics and dyes follow first-order kinetics concerning 4-NP/dye. Hence, the values of k_{app} for the catalytic reduction reaction are proportional to the catalyst surface area. Thus, it can be determined.[167]

$$BH_4^- + S \overset{k_{BH_4^-}}{\longleftrightarrow} BH_4^- \cdot S$$

$$BH_4^- + S \overset{adsorb}{\longrightarrow} BH_4^- \cdot S$$

$$BH_4^- \cdot S + H_2O \overset{k_H}{\longrightarrow} BO_2^- \cdot C + H \cdot S,$$

where $k_{BH_4^-}$ is the adsorption equilibrium constant for BH_4^- and k_H is the hydrolysis rate constant for BH_4^-, and S is the catalyst surface.
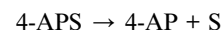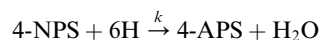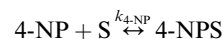
The reduction of 4-NP into 4-AP *via* an intermediate 4-hydroxyaminophenol can be represented as follows:

$$4\text{-NP} + S \overset{k_{4\text{-NP}}}{\longleftrightarrow} 4\text{-NPS}$$

$$4\text{-NPS} + 6H \overset{k}{\longrightarrow} 4\text{-APS} + H_2O$$

$$4\text{-APS} \rightarrow 4\text{-AP} + S$$

The adsorption and desorption processes of BH_4^- and 4-NP at the surface of the catalyst are fast and thus do not influence the kinetics of the reduction process. The slowest step, which is the rate-determining step, is the conversion of 4-NP into 4-AP by active hydrogen species.

The catalytic reduction of 4-NP by Ni(OH)$_2$@NSA-PANI nanocomposite catalyst followed the Langmuir–Hinshelwood mechanism, and the Ni(OH)$_2$ NPs on the NSA-PANI surface acted as electron-acceptors, which reversibly adsorbed hydride onto the NPs from NaBH$_4$, followed by adsorption of the substrate with the expulsion of hydrogen, thereby transferring surface-bound hydride to the –NO$_2$ group of nitro compounds in the rate-determining step of the reduction reaction. The hydrogen atoms on the surface of the nickel hydroxide in the Ni(OH)$_2$@NSA-PANI nanocomposite coordinate with d orbitals of Ni *via* 1s electron and form metal hydride bonds *via* chemisorption.[157] The catalytic reduction of the mechanism of 4-NP by PANI/Bi$_2$O$_3$ nanocomposite used Bi$_2$O$_3$ as the active centre, which transformed 4-NP into 4-AP *via* the formation of an intermediate 4-hydroxyaminophenol. The PANI acts as a stabilizer and capping agent preventing the agglomeration of Bi$_2$O$_3$ particles and acts as better hosts that suitably hold the Bi$_2$O$_3$ NPs.[117] The reduction of 4-NP by AgClNPs/PANI/D-Dex nanocomposite catalyst occurs on the active centre AgCl NPs, which

Fig. 8 4-NP reduction mechanism in the presence of polyaniline-based nanocomposite catalysts and reducing agent (BH_4^-).
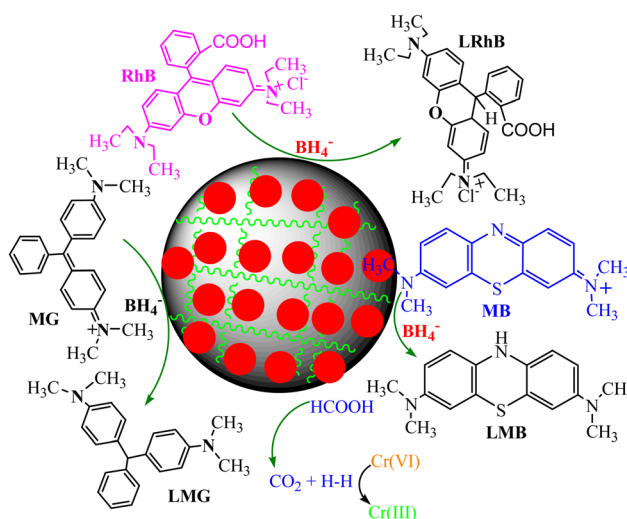

Fig. 9 Catalytic reduction process of various water pollutant polyaniline-based nanocomposite catalysts.

provides an electron transferring surface from an electron donor to the acceptor and requires hydrogen atoms for reduction of 4-NP to 4-AP *via* an intermediate 4-hydroxyaminophenol.[69]

The catalytic reduction mechanism of organic dyes and other pollutants in the presence of PANI-based nanocomposite catalysts and reducing agents is shown in Fig. 9. Dye molecules (MB, RhB, and MG dye) were adsorbed on the catalyst surface and received electrons and hydrogen ions from the reducing agent *via* the catalyst surface because they transform into nontoxic and colorless leuco forms, which desorb and regenerate catalysts that enter a fresh cycle of catalysis. The catalytic reduction mechanism of toxic Cr(VI) metal ions uses PANI-based nanocomposites in the presence of formic acid.[136,154] In the presence of a catalyst, formic acid produces hydrogen that interacts with Cr(VI) ions and transforms into Cr(III) ions.[136]

6.   Conclusion

The catalytic degradation of hazardous water pollutants, such as organic dyes, nitroaromatics, and metal ions, using heterogeneous catalysts is a facile, efficient, inexpensive, rapid, and greener method by which toxic materials can be transformed into less toxic or nontoxic under normal atmospheric conditions. Common heterogeneous nanocatalysts used for the decontamination of water pollutants or other catalysis reactions are metal-based nanoparticles. However, in the pure state, metal-based NPs demonstrate poor activity and stability due to aggregation. To reduce agglomeration and improve the surface area, catalytic activity, and stability, the catalysts can be immobilized with polymeric materials, especially conducting polymers, which provide support and cover shells to NPs. The application of PANI conducting polymers as supporting materials to metal-based NPs has gained wide attention. The prepared metal containing PANI-based nanocomposites *via* numerous techniques was effectively explored for the catalytic degradation of various water pollutants under ambient conditions. Using PANI as a matrix material, the heterogeneous catalyst suffers from recovery and reusability issues, which can be improved by introducing magnetic characteristics to PANI-based nanocomposites. Magnetic PANI-based nanocomposite catalysts with core–shell structures displayed good stability, recoverability, and activity in the catalysis reactions. In the magnetic core–shell, PANI-based composites with yolk–shell structures were used more efficiently in catalytic reactions due to their high surface characteristics, vacant area, and low density, and yolk–shell nanocomposites made of bimetallic nanoparticles exhibited higher reduction potential ability towards water pollutants. Among the various environmental pollutants, such as organic dyes, nitrophenols, and metal ions, nitrophenols, such as 4-NP, have wide industrial importance, but they exhibit serious mutagenic and hazardous impacts. Thus, the reduction of 4-NP into a less hazardous amino-product has numerous industrial applications. The catalytic degradation process of water pollutants, including nitro-aromatics, in the presence of heterogeneous catalysts follows pseudo-first-order kinetics in which the reaction rate depends on the surface area of the catalyst covered by the pollutant and reducing agent. In the reduction reaction, the catalyst acts as an electron relay surface through which electrons are transferred from the reducing agent (electron donor) to the pollutant (electron acceptor). Consequently, the pollutant molecules adsorbed on the catalyst surface are reduced to a nontoxic form. Hence, the synthesis of PANI-based nanocomposite heterogeneous catalysts with improved life span, stability, reusability, and recovery that can display effective reduction ability against a wide range of water pollutants is indispensable for sustainable and eco-friendly water purification techniques.

Data availability

No primary research results, software or code has been included and no new data were generated or analysed as part of this review.

Conflicts of interest

The author declares that he has no known competing financial interests.

Acknowledgements

References

1 S. L. Postel, G. C. Daily and P. R. Ehrlich, *Science*, 1996, **271**, 785–788.
2 K. N. Heck, S. Garcia-Segura, P. Westerhoff and M. S. Wong, *Chem. Res.*, 2019, **52**, 906–915, DOI: **10.1021/acs.accounts.8b00642**.
3 P. L. Meena, J. K. Saini, A. K. Surela, K. Poswal and L. K. Chhachhia, *Biomass Convers. Biorefin.*, 2024, **14**, 1711–1730, DOI: **10.1007/s13399-021-02267-2**.
4 P. L. Meena, *J. Geol. Soc. India*, 2022, **98**, 1455–1465, DOI: **10.1007/s12594-022-2193-9**.
5 S. Yadav, A. Yadav, N. Bagotia, A. K. Sharma and S. Kumar, *J. Water Process Eng.*, 2021, **42**, 102148.
6 Y. Wang, K. Wang and X. Wang, *J. Colloid Interface Sci.*, 2016, **466**, 178–185.
7 X. Li, H. Shi, K. Li and L. Zhang, *Front. Environ. Sci. Eng.*, 2015, **9**(6), 1076–1083.
8 Y. Zhang, Z. He, H. Wang, L. Qi, G. Liu and X. Zhang, *Front. Environ. Sci. Eng.*, 2015, **9**(5), 770–783.
9 J. Wang and Z. Bai, *Chem. Eng. J.*, 2017, **312**, 79–98.
10 S. Khamparia and D. K. Jaspal, *Front. Environ. Sci. Eng.*, 2017, **11**(1), 8.
11 P. Wang and M. C. Lo Irene, *Water Res.*, 2009, **43**, 3727–3734.
12 Z. Xiong, J. J. Ma, W. Ng, T. D. Waite and X. S. Zhao, *Water Res.*, 2011, **45**, 2095–2103.
13 H. Zhu, F. Xu, J. Zhao, L. Jia and K. Wu, *Environ. Sci. Pollut. Res. Int.*, 2015, **22**(18), 14299–14306.

14 J. Li, H. He, C. Hu and J. Zhao, *Front. Environ. Sci. Eng.*, 2013, **7**(3), 302–325.

15 Z. He, M. Hu and X. Wang, *Catal. Today*, 2018, **302**, 136–145.

16 X. Chu, G. Shan, C. Chang, Y. Fu, L. Yue and L. Zhu, *Front. Environ. Sci. Eng.*, 2016, **10**(2), 211–218.

17 S. Komathi, A. I. Gopalan, N. Muthuchamy and K. P. Lee, *RSC Adv.*, 2017, **7**(25), 15342–15351.

18 G. Saianand, A.-I. Gopalan, L. Wang, K. Venkatramanan, V. A. L. Roy, P. Sonar, D.-E. Lee and R. Naidu, *Environ. Technol. Innovat.*, 2022, **28**, 102698, DOI: 10.1016/j.eti.2022.102698.

19 F. F. Runge, *Ann. Phys. Chem.*, 1834, **107**, 65.

20 J. Stejskal and R. G. Gilbert, *Pure Appl. Chem.*, 2002, **74**, 857–867.

21 G. Ciric-Marjanovic, *Synth. Met.*, 2013, **177**, 1–47.

22 S. Bhadra, D. Khastgir, N. K. Singha and J. H. Lee, *Prog. Polym. Sci.*, 2009, **34**, 783–810.

23 D. D. Zhou, X. T. Cui, A. Hines and R. J. Greenberg, In *Implantable Neural Prostheses 2: Techniques and Engineering Approaches*, Springer, New York, NY, USA, 2009, pp. 217–252.

24 H. T. Das, S. Dutta, R. Beura and N. Das, *Environ. Sci. Pollut. Res.*, 2022, **29**, 49598–49631.

25 S. Bhadra, N. K. Singha and D. Khastgir, *Polym. Int.*, 2007, **56**, 919–927.

26 A. A. Syed and M. K. Dinesan, *Talanta*, 1991, **38**, 815–837.

27 J. Gong, X.-J. Cui, Z.-W. Xie, S.-G. Wang and L.-Y. Qu, *Synth. Met.*, 2002, **129**, 187–192, DOI: 10.1016/S0379-6779(02)00052-8.

28 T. Abdiryim, Z. Xiao-Gang and R. Jamal, *Mater. Chem. Phys.*, 2005, **90**, 367–372, DOI: 10.1016/j.matchemphys.2004.10.036.

29 Y. Chen, E. T. Kang and K. G. Neoh, *Appl. Surf. Sci.*, 2002, **185**, 267–276, DOI: 10.1016/S0169-4332(01)00817-0.

30 A. F. Diaz and J. A. Logan, *J. Electroanal. Chem.*, 1980, **111**, 111–114.

31 S. K. Mondal, K. R. Prasad and N. Munichandraiah, *Synth. Met.*, 2005, **148**, 275.

32 C. Nastase, F. Nastase, A. Dumitru, M. Ionescu and I. Stamatin, *Compos. Appl. Sci. Manuf.*, 2005, **36**, 481–485.

33 X. Jing, Y. Y. Wang, D. Wu and J. P. Qiang, *Ultrason. Sonochem.*, 2007, **14**, 75–80.

34 N. Kobayashi, K. Teshima and R. Hirohashi, *J. Mater. Chem.*, 1998, **8**, 497–506.

35 N. Kuramoto and A. Tomita, *Synth. Met.*, 1997, **88**, 147–151.

36 S. Xing, C. Zhao, S. Jing and Z. Wang, *Polymer*, 2006, **47**, 2305–2313.

37 J. Y. Kim, J. H. Lee and S. J. Kwon, *Synth. Met.*, 2007, **157**, 336–342.

38 Q. Guo, C. Yi, L. Zhu, Q. Yang and Y. Xie, *Polymer*, 2005, **46**, 3185–3189.

39 P. Dallas, D. Stamopoulos, N. Boukos, V. Tzitzios, D. Niarchos and D. Petridis, *Polymer*, 2007, **48**, 3162–3169.

40 J. Chen, D. Chao, X. Lu and W. Zhang, *Mater. Lett.*, 2007, **61**, 1419–1423.

41 R. V. Parthasarathy and C. R. Martin, *Chem. Mater.*, 1994, **6**, 1627–1632.

42 J. Choi, S. J. Kim, J. Lee, J. H. Lim, S. C. Lee and K. J. Kim, *Electrochem. Commun.*, 2007, **9**, 971–975.

43 S. Kobayashi and A. Makino, *Chem. Rev.*, 2009, **109**, 5288–5353.

44 V. R. Gowariker, N. V. Viswanathan and J. Sreedhar, *Polymer Science*, New Delhi, India, New Age International (P) Limited, 1996, 73.

45 J. Stejskal, I. Sapurina, J. Prokeš and J. Zemek, *Synth. Met.*, 1999, **105**, 195–202, DOI: 10.1016/S0379-6779(99)00105-8.

46 N. Kumari Jangid, S. Jadoun and N. Kaur, *Eur. Polym. J.*, 2020, **125**, 109485, DOI: 10.1016/j.eurpolymj.2020.109485.

47 J. L. Camalet, J. C. Lacroix, S. Aeiyach, K. Chane-Ching and P. C. Lacaze, *Synth. Met.*, 1998, **93**, 133–142.

48 G. Mengoli, M. T. Munari and C. Folonari, *J. Electroanal. Chem.*, 1981, **124**, 237–246.

49 E. W. Paul, A. J. Ricco and M. S. Wrighton, *J. Phys. Chem.*, 1985, **89**, 1441–1447.

50 R. L. Hand and R. F. Nelson, *J. Electrochem. Soc.*, 1978, **125**, 1059–1069.

51 A. M. P. Hussain and A. Kumar, *Bull. Mater. Sci.*, 2003, **26**, 329–334.

52 L. R. Vargas, A. K. Poli, R. D. C. L. Dutra, C. B. D. Souza, M. R. Baldan and E. S. Gonçalves, *J. Aero. Technol. Manag.*, 2017, **9**, 29–38.

53 S. Goswami, S. Nandy, E. Fortunato and R. Martins, *J. Solid State Chem.*, 2023, **317**, 123679, DOI: 10.1016/j.jssc.2022.123679.

54 M. J. Silva, J. Gomes, P. Ferreira and R. C. Martins, *Water*, 2022, **14**(5), 1–34, DOI: 10.3390/w14050825.

55 M. H. Alhaji, K. Sanaullah, A. Khan, A. Hamza, A. Muhammad, M. S. Ishola, A. R. H. Rigit and S. A. Bhawani, *Int. J. Environ. Sci. Technol.*, 2017, **14**(9), 2039–2052.

56 A. Bouarioua and M. Zerdaoui, *J. Environ. Chem. Eng.*, 2017, **5**(2), 1565–1574.

57 C. W. Lin, S. Xue, C. Ji, S. C. Huang, V. Tung and R. B. Kaner, *Nano Lett.*, 2021, **21**(9), 3699–3707, DOI: 10.1021/acs.nanolett.1c00968.

58 H. S. Zakria, M. H. D. Othman, R. Kamaludin, S. H. S. A. Kadir, T. A. Kurniawan and A. Jilani, *RSC Adv.*, 2021, **11**(12), 6985–7014.

59 N. K. Jangid, S. Jadoun, A. Yadav, M. Srivastava and N. Kaur, *Polym. Bull.*, 2021, **78**, 4743–4777, DOI: 10.1007/s00289-020-03318-w.

60 X. Liu and L. Cai, *Appl. Surf. Sci.*, 2019, **483**, 875–887.

61 K. Luo, X. Guo, N. Shi and C. Sun, *Synth. Met.*, 2005, **151**, 293–296.

62 A. A. Athawale, S. V. Bhagwat and P. P. Katre, *Sens. Actuators, B*, 2006, **114**, 263–267.

63 A. Arzac, G. P. Leal, R. Fajgar and R. Tomovska, *Part. Part. Syst. Char.*, 2014, **31**, 143–151.

64 S. Mandal, S. K. Saha and P. Chowdhury, *Int. J. Curr. Microbiol. Appl. Sci.*, 2017, **6**, 2309–2321.

65 A. Asatekin, M. C. Barr, S. H. Baxamusa, K. K. Lau, W. Tenhaeff, J. Xu and K. K. Gleason, *Mater. Today*, 2010, **13**, 26–33.

66 D. Bharti and S. P. Tiwari, *Synth. Met.*, 2016, **221**, 186–191.

67 M. R. U. D. Biswas, K. Y. Cho, C.-H. Jung and W.-C. Oh, *Process Saf. Environ. Prot.*, 2015, **126**, 348–355.

68 X. Zhu, Z. Song, Z. Wang, W. Liu, B. Hong, J. Bao, C. Gao and S. Sun, *Appl. Catal., B*, 2020, **274**, 119010.

69 E. Prabakaran and K. Pilla, *J. Mol. Liq.*, 2019, **283**, 6–29, DOI: **10.1016/j.molliq.2019.03.014**.

70 S. Liu, B. Yu, S. Wang, Y. Shen and H. Cong, *Adv. Colloid Interface Sci.*, 2020, **281**, 102165.

71 K. Dayanidhi, P. Vadivel, S. Jothi and N. S. Eusuff, *J. Environ. Manage.*, 2020, **271**, 110962.

72 M. E. Kalkan, *Colloid Interface Sci. Commun.*, 2020, **34**(20), 100222, DOI: **10.1016/j.colcom.2019.100222**.

73 R. Das, V. S. Sypu, H. K. Paumo, M. Bhaumik, V. Maharaj and A. Maity, *Appl. Catal., B*, 2019, **244**, 546–558.

74 M. Nasrollahzadeh, M. Sajjadi, J. Dadashi and H. Ghafuri, *Adv. Colloid Interface Sci.*, 2020, **276**, 102103.

75 S. A. Akintelu, A. S. Folorunso, F. A. Folorunso and A. K. Oyebamiji, *Heliyon*, 2020, **6**, e04508.

76 N. Tian, Z.-Y. Zhou, S.-G. Sun, Y. Ding and Z. L. Wang, *Science*, 2007, **316**, 732735.

77 D. Astruc, *Nanoparticles and Catalysis, Transition-Metal Nanoparticles in Catalysis: from Historical Background to the State-Of-The Art*, Wiley-VCH, Weinheim, 2008.

78 M. Chen, P. Liu, C. Wang, W. Ren and G. Diao, *New J. Chem.*, 2014, **38**, 4566–4573, DOI: **10.1039/C4NJ00806E**.

79 M. R. Nabid, Y. Bide, N. Ghalavand and M. Niknezhad, *Appl. Organomet. Chem.*, 2014, **28**(6), 389–395, DOI: **10.1002/aoc.3133**.

80 H. Mou, C. Song, Y. Zhou, B. Zhang and D. Wang, *Appl. Catal., B*, 2018, **221**, 565–573.

81 O. Ramirez, S. Bonardd, C. Saldias, D. Radic and A. Leiva, *ACS Appl. Mater. Interfaces*, 2017, **9**, 16561–16570.

82 M. Bhaumik, A. Maity and H. G. Brink, *J. Colloid Interface Sci.*, 2022, **611**, 408–420.

83 P. Mondal, C. Guo and J. L. Yarger, *Arab. J. Chem.*, 2020, **13**, 4009–4018.

84 L. Sun, L. Jiang, J. Zhang, T. Murayama, M. Zhang, Y. Zheng, H. Su and C. Qi, *Top. Catal.*, 2021, **64**, 215–223, DOI: **10.1007/s11244-020-01385-x**.

85 Y. Wang, Y. Shen, A. Xie, S. Li, X. Wang and Y. Cai, *J. Phys. Chem. C*, 2010, **114**, 4297–4301.

86 M. Ma, Q. Zhang, D. Yin, J. Dou, H. Zhang and H. Xu, *Catal. Commun.*, 2012, **17**, 168–172.

87 K. D. Vorlop and T. Tacke, *Chemieingenieurtechnik*, 1989, **61**(10), 836–837.

88 Y. B. Yin, S. Guo, K. N. Heck, C. A. Clark, C. L. Conrad and M. S. Wong, *ACS Sustain. Chem. Eng.*, 2018, **6**(9), 11160–11175.

89 J. Liu and J. Gao, *Environ. Sci. Eng.*, 2023, **17**(2), 26, DOI: **10.1007/s11783-023-1626-z**.

90 Y. Zhang, P. Zhu, G. Li, W. Wang, L. Chen, D. D. Lu, R. Sun, F. Zhou and C. Wong, *Nanoscale*, 2015, **7**, 13775–13783.

91 P. Boomi, H. G. Prabu and J. Mathiyarasu, *Eur. J. Med. Chem.*, 2014, **72**, 18–25.

92 X. Sun, H. Su, Q. Lin, C. Han, Y. Zheng, L. Sun and C. Qi, *Appl. Catal., A*, 2016, **527**, 19–29.

93 A. Pourjavadi, M. Doroudian, A. Abedin-Moghanaki and C. Bennett, *Appl. Organomet. Chem.*, 2017, **31**, e3881.

94 J. Lee, J. C. Park and H. Song, *Adv. Mater.*, 2008, **20**(8), 1523–1528.

95 V. Georgakilas, D. Gournis, V. Tzitzios, L. Pasquato, D. M. Guldi and M. Prato, *J. Mater. Chem.*, 2007, **17**, 2679–2694.

96 C. Xu, X. Wang and J. Zhu, *J. Phys. Chem. C*, 2008, **112**, 19841–19845.

97 P. L. Meena, J. K. Saini and A. K. Surela, *Inorg. Chem. Commun.*, 2023, **152**, 110688, DOI: **10.1016/j.inoche.2023.110688**.

98 B. Zhang, T. Cai, S. Li, X. Zhang, Y. Chen, K. G. Neoh, E. T. Kang and C. Wang, *J. Mater. Chem. C*, 2014, **2**, 5189–5197.

99 J. Han, S. Lu, C. Jin, M. Wang and R. Guo, *J. Mater. Chem. A*, 2014, **2**, 13016.

100 J. Han, R. Chen, M. Wang, S. Lu and R. Guo, *Chem. Commun.*, 2013, **49**, 11566–11568.

101 V. Divya and M. V. Sangaranarayanan, *Eur. Polym. J.*, 2012, **48**, 560.

102 Z. Lu, W. Dai, B. Liu, G. Mo, J. Zhang, J. Ye and J. Ye, *J. Colloid Interface Sci.*, 2018, **525**, 86.

103 Z. Zhang, Y. Jiang, M. Chi, Z. Yang, G. Nie, X. Lu and C. Wang, *Appl. Surf. Sci.*, 2016, **363**, 578–585.

104 J. Yu, W. Guo, M. Yang, Y. Luan, J. Tao and X. Zhang, *Sci. China Chem.*, 2014, **57**, 1211–1217.

105 N. H. Mack, J. A. Bailey, S. K. Doorn, C. A. Chen, H. M. Gau, P. Xu, D. J. Williams, E. A. Akhadov and H. L. Wang, *Langmuir*, 2011, **27**, 4979–4985.

106 J. Han, L. Li and R. Guo, *Macromolecules*, 2010, **43**, 10636–10644.

107 S. K. Arya, A. Dey and S. Bhansali, *Biosens. Bioelectron.*, 2011, **28**, 166–173.

108 H. H. Saleh, Z. I. Ali and T. A. Afify, *Adv. Polym. Technol.*, 2016, **35**, 335.

109 S. K. Pillalamarri, F. D. Blum, A. T. Tokuhiro and M. F. Bertino, *Chem. Mater.*, 2005, **17**, 5941.

110 K. Takemura, J. Satoh, J. Boonyakida, S. Park, A. D. Chowdhury and E. Y. Park, *J. Nanobiotechnol.*, 2020, **18**, 152.

111 N. Shoaie, M. Forouzandeh and K. Omidfar, *Microchim. Acta*, 2018, **185**, 217.

112 P. Chakraborty, Y.-A. Chien, T.-F. M. Chang, M. Sone and T. Nakamoto, *Sensors*, 2020, **20**, 13.

113 W. Jin, X. Huang, H. Cheng, T. Xu, F. Wang, X. Guo, Y. Wu, Y. Ying, Y. Wen and H. Yang, *Appl. Surf. Sci.*, 2019, **483**, 489.

114 G. N. Abdelrasoul, F. Pignatelli, I. Liakos, R. Cingolani and A. Athanassiou, *Composites, Part B*, 2018, **149**, 178.

115 G. Chang, Y. Luo, W. Lu, X. Qin, A. M. Asiri, A. O. Al-Youbib and X. Sun, *Catal. Sci. Technol.*, 2012, **2**, 800–806.

116 K. M. Manesh, A. I. Gopalan, K. P. Lee and S. Komathi, *Catal. Commun.*, 2010, **11**, 913–918.

117 K. J. Kshirasagar, U. S. Markad, A. Saha, K. K. K. Sharma and G. K. Sharma, *Mater. Res. Express*, 2017, **4**, 025015, DOI: 10.1088/2053-1591/aa5947.

118 G. Joseph, D. Pinheiro, M. K. Mohan and S. D. K. R. Pai, *Polym. Bull.*, 2023, **80**, 8467–8481, DOI: 10.1007/s00289-022-04457-y.

119 H. Huang, C. Li, Q. Zhang, J. Huang, J. Ji, Y. Liu and L. Li, *Polym. Compos.*, 2023, **44**(11), 7674–7686, DOI: 10.1002/pc.27655.

120 G. Wang, S. Yuan, Z. Wu, W. Liu, H. Zhan, Y. Liang, X. Chen, B. Ma and S. Bi, *Appl. Organomet. Chem.*, 2019, e5159, DOI: 10.1002/aoc.5159.

121 Y. Chen, S. Lu, W. Liu and J. Han, *Colloid Polym. Sci.*, 2015, **293**, 2301–2309.

122 S. P. Deshmukh, A. G. Dhodamani, S. M. Patil, S. B. Mullani, K. V. More and S. D. Delekar, *ACS Omega*, 2020, **5**, 219–227.

123 P. L. Meena and J. K. Saini, *Results Chem.*, 2023, **5**, 100764, DOI: 10.1016/j.rechem.2023.100764.

124 T. Fatima, S. Husain and M. Khanuja, *Chem. Eng. J. Adv.*, 2022, **12**, 100373.

125 J. Ma, J. Dai, Y. Duan, J. Zhang, L. Qiang and J. Xue, *Renewable Energy*, 2020, **56**, 1008–1018.

126 P. L. Meena and A. K. Surela, *Reference Module in Materials Science and Materials Engineering*, 2024, DOI: 10.1016/B978-0-323-95486-0.00003-X.

127 P. L. Meena, J. K. Saini, A. K. Surela, B. Mordhiya, L. Kumari Chhachia and K. S. Meena, *ChemistrySelect*, 2023, **8**, e202300724, DOI: 10.1002/slct.202300724.

128 P. L. Meena, J. K. Saini, A. K. Surela and K. Poswal, *Holist. Approach Environ.*, 2022, **12**(4), 131–143, DOI: 10.33765/thate.12.4.1.

129 M. Alhoshan, J. Alam, A. K. Shukla and A. A. Hamid, *J. Mater. Res. Technol.*, 2023, **4**, 6034–6047, DOI: 10.1016/j.jmrt.2023.04.200.

130 J. Alam, A. K. Shukla, M. A. Ansari, F. A. A. Ali and M. Alhoshan, *Membranes*, 2021, **11**(1), 25, DOI: 10.3390/membranes11010025.

131 I. Chajanovsky and R. Y. Suckeveriene, *Processes*, 2020, **8**(11), 1503, DOI: 10.3390/pr8111503.

132 C. Zhang, S. Govindaraju, K. Giribabu, Y. S. Huh and K. Yun, *Sens. Actuators, B*, 2017, **252**, 616–623.

133 Y. Kong, T. Wu, D. Wu, Y. Zhang, Y. Wang, B. Du and Q. Wei, *Anal. Methods*, 2018, **10**, 4784–4792, DOI: 10.1039/C8AY01245H.

134 A. Khan, A. A. P. Khan, M. M. Rahman, A. M. Asiri, Inamuddin, K. A. Alamry and S. A. Hameed, *Appl. Surf. Sci.*, 2018, **433**, 696–704.

135 S. Zhao, L. Huang, T. Tong, W. Zhang, Z. Wang, J. Wang and S. Wang, *Environ. Sci.: Water Res. Technol.*, 2017, **3**, 710–719, DOI: 10.1039/C6EW00332J.

136 K. Sivaranjan, O. Padmaraj, J. Santhanalakshmi, M. Sathuvan, A. Sathiyaseelan and S. Sagadevan, *Sci. Rep.*, 2020, **10**, 2586, DOI: 10.1038/s41598-020-59491-5.

137 H. Gul, A.-H. A. Shah, U. Krewer and S. Bilal, *Nanomaterials*, 2020, **10**, 1.

138 Y. Chen, S. Lu, W. Liu and J. Han, *Colloid Polym. Sci.*, 2015, **293**, 2301–2309.

139 Y. Chen, L. Li, L. Zhang and J. Han, *Colloid Polym. Sci.*, 2018, **296**, 567–574, DOI: 10.1007/s00396-018-4276-0.

140 Y. Li, Y. Hu, S. Ye, Y. Wu, C. Yang and L. Wang, *New J. Chem.*, 2016, **40**, 10398.

141 X. Qiao, X. Liu, X. Li and S. Xing, *New J. Chem.*, 2015, **39**, 8588–8593.

142 B. Zhang, B. Zhao, S. Huang, R. Zhang, P. Xu and H. L. Wang, *CrystEngComm*, 2012, **14**, 1542–1544.

143 M. Khani, R. Sammynaiken and L. D. Wilson, *Catalysts*, 2023, **13**, 465, DOI: 10.3390/catal13030465.

144 P. L. Meena, L. K. Chhachhia and A. K. Surela, *J. Mol. Struct.*, 2024, **1303**, 137575, DOI: 10.1016/j.molstruc.2024.137575.

145 P. L. Meena, A. K. Surela, K. Poswal, J. K. Saini and L. K. Chhachhia, *Environ. Sci. Pollut. Res.*, 2022, **29**, 79253–79271, DOI: 10.1007/s11356-022-21435-z.

146 P. L. Meena, A. K. Surela, K. Poswal, J. K. Saini and L. K. Chhachhia, *Biomass Convers. Biorefin.*, 2024, **14**, 3793–3809, DOI: 10.1007/s13399-022-02605-y.

147 P. L. Meena, K. Poswal, A. K. Surela, B. Mordhiya and K. S. Meena, *Environ. Sci. Pollut. Res.*, 2023, **30**, 68770–68791, DOI: 10.1007/s11356-023-27215-7.

148 K. Shang, B. Sun, J. Sun, J. Li and S. Ai, *New J. Chem.*, 2013, **37**, 2509–2514.

149 Md. Amir, U. Kurtan, A. Baykal and H. Sözeri, *J. Mater. Sci. Technol.*, 2016, **32**(2), 134–141.

150 Y. Zhu, X. Zhou, D. Chen, F. Li, T. Xue and A. S. Farag, *Sci. China Technol. Sci.*, 2017, **60**, 749–757, DOI: 10.1007/s11431-016-0663-0.

151 C. Jin, J. Han, F. Chu, X. Wang and R. Guo, *Langmuir*, 2017, **33**(18), 4520–4527.

152 M. S. Najafinejad, P. Mohammadi, M. M. Afsahi and H. Sheibani, *Mater. Sci. Eng. C*, 2019, **98**, 19–29.

153 M. E. Mahmoud, M. F. Amira, M. E. Abouelanwar and S. M. Seleim, *J. Mol. Liq.*, 2020, **299**, 112192, DOI: 10.1016/j.molliq.2019.112192.

154 B. Vellaichamy, P. Periakaruppan and B. Nagulan, *ACS Sustainable Chem. Eng.*, 2017, **5**, 9313–9324, DOI: 10.1021/acssuschemeng.7b02324.

155 L. Sun, X. Sun, Y. Zheng, Q. Lin, H. Su and C. Qi, *Synth. Met.*, 2017, **224**, 1–6.

156 J. Ma, H. Deng, Z. Zhang, L. Zhang, Z. Qin, Y. Zhang, L. Gao and T. Jiao, *Colloids Surf., A*, 2022, **632**(2), 127774, DOI: 10.1016/j.colsurfa.2021.127774.

157 V. S. Sypu, M. Bhaumik, K. Raju and A. Maity, *J. Colloid Interface Sci.*, 2021, **581**, 979–989.

158 M. M. Ayad, W. A. Amer, M. G. Kotp, I. M. Minisy, A. F. Rehab, D. Kopecky and P. Fitl, *RSC Adv.*, 2017, **7**, 18553.

159 M. M. Ayad, W. A. Amer and M. G. Kotp, *Mol. Catal.*, 2017, **439**, 72–80.

160 Z. Gan, A. Zhao, M. Zhang, W. Tao, H. Guo, Q. Gao, R. Mao and E. Liu, *Dalton Trans.*, 2013, **42**, 8597–8605, DOI: 10.1039/C3DT50341K.

161 J. Liu, S. Z. Qiao, S. Budi Hartono and G. Lu, *Angew. Chem., Int. Ed.*, 2010, **49**, 4981–4985.

162 L. Sun, Z. Yin, J. Zhang, X. Ren, M. Zhang, W. Song, Z. Xu and C. Qi, *Mol. Catal.*, 2022, **525**, 112362.

163 L. Yu, D. Li, Z. Xu and S. Zheng, *Chemosphere*, 2023, **310**(10), 136685, DOI: **10.1016/j.chemosphere.2022.136685**.

164 C. Sun, N. Deng, H. An, H. Cui and J. Zhai, *Chemosphere*, 2015, **141**, 243–249.

165 B. Al-saida, W. A. Amer, E. E. Kandyel and M. M. Ayad, *J. Photochem. Photobiol., A*, 2020, **392**, 112423, DOI: **10.1016/j.jphotochem.2020.112423**.

166 M. I. Din, R. Khalid, Z. Hussain, T. Hussain, A. Mujahid, J. Najeeb and F. Izhar, *Crit. Rev. Anal. Chem.*, 2020, **50**(4), 322–338, DOI: **10.1080/10408347.2019.1637241**.

167 A. Serrà, R. Artal, M. Pozo, J. Garcia-Amoros and E. Gom, *Catalysts*, 2020, **10**, 458, DOI: **10.3390/catal10040458**.

168 Z. M. El-Bahy, *Appl. Catal., A*, 2013, **468**, 175–183.

169 S. R. Thawarkar, B. Thombare, B. S. Mundec and N. D. Khupse, *RSC Adv.*, 2018, **8**, 38384–38390.

170 J. Y. Shen, X. P. Xu, X. B. Jiang, C. X. Hua, L. B. Zhang, X. Y. Sun, J. S. Li, Y. Mu and L. J. Wang, *Water Res.*, 2014, **67**, 11–18.

171 S. R. Thawarkar, B. Thombare, B. S. Munde and N. D. Khupse, *RSC Adv.*, 2018, **8**, 38384.

172 M. Kohantorabi and M. R. Gholami, *Ind. Eng. Chem. Res.*, 2017, **56**, 1159–1167, DOI: **10.1021/acs.iecr.6b04208**.

173 N. Bingwa and R. Meijboom, *J. Phys. Chem. C*, 2014, **118**, 19849–19858, DOI: **10.1021/jp505571p**.